

AD-A122 331


THEORY OF MANY-BODY EFFECTS IN SUB-MICROELECTRONIC
SYSTEMS(U) CHELSEA COLL LONDON (ENGLAND) DEPT OF
PHYSICS L A DISSADO ET AL. OCT 82 DAJA37-81-C-0814

1/1

UNCLASSIFIED

F/G 9/3

NL

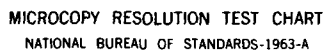
														

END

FIGURE

1

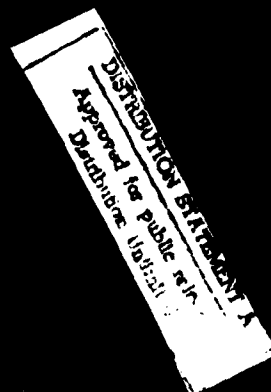
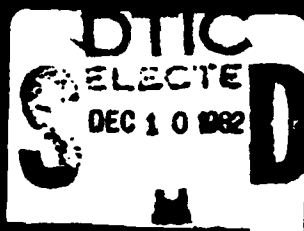
010



MICROCOPY RESOLUTION TEST CHART
NATIONAL BUREAU OF STANDARDS-1963-A

AD A 122331

DIC FILE COPY



10
Theory of Many-Body Effects in
Sub-Microelectronic Systems.
Final Technical Report

by
L. A. Dissado and R. M. Hill
November 1981 - October 1982

DTIC
DEC 10 1982
H

United States Army
EUROPEAN RESEARCH OFFICE OF THE U. S. ARMY
London England
Contract Number DAJA37 - 81 - C-0814
Chelsea College

The research reported in this document has been made possible through the support and sponsorship of the U.S. Government through its European Research Office of the U.S. Army.

DISTRIBUTION STATEMENT A

Approved for public release;
Distribution Unlimited

Theory of Many-Body Effects in Sub-Microelectronic
Systems II

Anomalous Low Frequency Dispersion

A near D.C. conductivity in low dimensional Materials.

L. A. Dissado and R. M. Hill

Chelsea College, Department of Physics, University of
London, Pulton Place, London SW6 5PR.

Abstract

A new interpretation of the anomalous dispersion process which is observed at low frequencies is presented which is based on a realistic description of the structural ordering and fluctuation in carrier dominated dielectrics. It is shown that this form of response occurs for systems of low spatial dimensionality and generates a sample-size dependent conductivity. The relationship of the mechanism to that of power law noise in electrical systems is identified and the structural interpretation explored. Particular features of hydrogen bonded systems are described in which the dispersion is likely to be important in a biological context. It is pointed out that the process is directly relevant to solid-state batteries such as those based on fast-ion conductors such as β -alumina.

Accession For	
NTIS GSA&I	<input checked="" type="checkbox"/>
DTIC TAB	<input type="checkbox"/>
Unannounced	<input type="checkbox"/>
Justification	<i>Per</i>
<i>For Sample</i>	
By	
Distribution/	
Availability Codes	
Dist	Avail and/or Special
<i>A</i>	



1. Introduction

In the previous report (Dissado and Hill, 1982) the effect of sample size in the macroscopic range was investigated in ferroelectric type materials as specific examples of bound charge, dielectrically active, systems. In the present study the complementary case of the effects of sample size in almost free carrier systems have been investigated. It is shown that the anomalous low frequency dispersion which is invariably observed in quasi-free ion carrier systems such as the Hollandites and β -alumina (Jonscher, 1978), does show characteristic size effects which can appear as a sample size dependent quasi-D.C. conductivity. Although these effects have only been characterised for ionic carriers it is argued that similar effects can occur in low dimensionality systems for electron carriers but will occur on much shorter time scales.

The dielectric response of a solid can be characterised by the dependence of the complex susceptibility, $\chi(\omega) = \chi'(\omega) - i\chi''(\omega)$, on the frequency, ω , and on the external variables such as temperature, pressure, humidity, etc. In general a peak is observed in the frequency dependence of the loss component $\chi''(\omega)$ together with a dielectric increment in the real component, $\chi'(\omega)$, corresponding to a relaxation process (McCrum et al., 1967). Typically such loss peaks have a non-Debye shape (Jonscher, 1975, 1977; Hill, 1981a) which is given by

$$\chi'(\omega) \propto \chi''(\omega) \propto \omega^{-(1-n)} \quad ; \quad \omega > \omega_p \quad (1a)$$

$$\text{and} \quad \chi''(\omega) = \chi(0) - a \cdot \chi'(\omega) \propto \omega^{+m} \quad ; \quad \omega < \omega_p \quad (1b)$$

where a is a constant and $\chi(0)$ is the susceptibility at zero frequency. The constants m and n lie between zero and unity and ω_p is the relaxation rate and may be identified with the frequency of maximum loss. A consequence of the high frequency behaviour of equation (1a) is that the ratio $\chi''(\omega)/\chi'(\omega)$ is independent of frequency (Cole and Cole, 1941; Jonscher, 1975) and is given by

$$\chi''(\omega)/\chi'(\omega) = \cot(n\pi/2) \quad (2)$$

However Jonscher (1978) has identified a second class of behaviour in which the frequency dependence of equation (1a) obtains through a transition from a small value of the index n at low frequencies to a different, and larger, value beyond a characteristic frequency ω_c , as shown in figure 1. Relationship (2) is obeyed in both the high and low frequency limits with the appropriate value of the index n . Neither frequency range has yet been observed to form part of a loss peak, furthermore $\chi(\omega)$ has been shown to be normalisable (Hill, 1978) with respect to variations in ω_c due to changes in temperature (Jonscher, 1978) and measuring field (Jonscher, Meca and Millany, 1979) in a similar manner to a loss characteristic (Ferry, 1970; Hill, 1978). The conditions for this to be possible should ω_c simply represent the point of overlap of two characteristics are very restrictive, namely that the susceptibility increment and characteristic frequency for each process should behave in an identical fashion with respect to variations in temperature and field, while yet being different in magnitude.

Thus this type of behaviour can best be regarded as a feature in its own right, and since it is the lowest frequency process observable dielectrically it has been termed the anomalous low frequency dispersion by Jonscher (1978). For convenience we define the value of $(1-n)$ in the lower frequency range to be p , and observe from the literature quoted that p lies in the range 0.7 to 1.0.

When the available frequency range only extends down to the dotted line in figure 1 the phenomena may be confused with the onset of D.C. conduction, for which

$$\chi'(\omega) = \text{constant} \quad \left| \quad \omega \rightarrow 0 \quad (3a) \right.$$

$$\chi''(\omega) \propto \sigma_{DC}/\omega \quad (3b)$$

with σ_{DC} the frequency independent D.C. conductivity. This behaviour is indicated by the light dotted curves in figure 1. Whilst the presence of a D.C. component cannot be ruled out the validity of relationship (2) in the extremely low frequency region effectively negates this as an explanation of the dispersion process. Similarly the Maxwell-Wagner effect (Maxwell, 1954; Wagner, 1914) predicts a limiting behaviour of the form of relationship (3) but with a higher frequency region in which

$$\chi''(\omega) \propto \omega^{-1} \quad \text{and} \quad \chi'(\omega) \propto \omega^{-2}$$

with the ratio of the imaginary and real components proportional to the frequency.

It has been proposed (Pollak and Geballe, 1961) that the high frequency portion of the anomalous dispersion can be described in terms of variable range hopping of carriers with values of n estimated to lie between 0.5 and 1.0 (Austin and Mott, 1969; Hill 1977). This model however offers no convincing explanation of the lower frequency dispersion which is a major feature of the response. A modified version of the model predicts a temperature dependence of n (Elliot, 1977) which is rarely, if ever, observed (Frost and Jonscher, 1975; Hill 1981a). Clearly such an explanation is partial at best. Jonscher (1977) has suggested that both regions of the anomalous response should be regarded as examples of the power law response common to all dielectrics, for which an explanation was suggested by Ngai et.al. (1979) in terms of a cooperative, many-body, model. It was suggested that the two regions of behaviour could be regarded as resulting from independent processes, although the nature of the difference was not specified. Furthermore in a few cases (Jonscher, 1978) the power law of the anomalous low frequency dispersion undergoes a further modification at the lowest frequencies to a characteristic with a value of p of one half. This latter fact cannot be explained on the basis of a third independent process, since such a process would not be observable in the presence of the dispersion with p close to unity. Such behaviour, where it occurs, must be regarded as the extremely low limit of the anomalous dispersion, and the power law exponent of 0.5 strongly suggests that it is determined by independent particle diffusion.

The full explanation of this class of dielectric response therefore seems likely to involve a composite process whose component parts can be identified with dynamical possibilities inherent in the material structure, in a similar manner to that of the loss peak (Dissado and Hill, 1979; Dissado, 1982), and possessing the observed limiting particle diffusion behaviour. We propose here that these criteria can be met by a model based on the concept of

a cluster of quasi-mobile charges possessing partial structural regularity, for which the model of Ngai et.al. (1979) is a particular case of a more general description which leads to a power law response (Halperin et.al., 1972; Binder et.al., 1975; Patashinskii and Pokrovskii, 1979). In the following sections we intend to identify the necessary elements for this model in the systems that produce this class of response and delineate the manner in which they contribute to the combined behaviour. During this exposition the connection with other electrical phenomena such as electrical noise (Gupta, 1977; Hill et.al., 1981) and D.C. conduction will become apparent.

2. Conditions necessary for Low Frequency Dispersion

The class of response identified above as anomalous low frequency dispersion has been observed in a wide range of materials of considerably different chemical nature. These include fast ion conductors such as Hollandite (Jonscher, 1978), ionic glasses (Jonscher and Frost, 1976; Doyle, 1981), wetted proteins (Jonscher 1978; Eden et.al., 1980), polymers (Bodiakan, 1982), solid nickel suspension (Ramdeen, 1981), humid sand (Shahidi et.al., 1975) and stearic acid films (Jonscher et.al., 1979). A comparison between the response of humid sand and sand/water mixture revealed that the dispersion is associated with the water present as an adsorbate. Since the catalytic activity of the solid nickel suspension depended upon the adsorption of molecules it is likely that in this case the effect also relies on the presence of water as an adsorbate. Furthermore the observation of the low frequency response in hydrated proteins has been strongly linked with the filling of secondary hydration sites (Eden et.al., 1980). In the case of polymers it is known that water diffuses into materials relatively easily (Auckland and Cooper, 1974) and adsorption may occur at the interface between the crystalline and amorphous regions such as spherulite and lamella surfaces (Barham and Keller, 1977). It therefore seems probable that the observation of the dispersion in all hydrated samples is a consequence of the formation of adsorbed water layers on the interior surfaces of one of the components of a heterogeneous material (Jonscher, 1978).

Although ionic materials such as Hollandite possess a distinctly different structural nature from that of the hydrated systems there are some significant similarities. In the Hollandites the crystal structure forms channels through which a migrating ion may pass to give D.C. conduction. These channels are one-dimensional in the Hollandites and are partially occupied with K^+ ions (Reau et.al., 1977; Jonscher et.al., 1979). The surrounding crystal structure creates a sinusoidal potential surface along the channels with minima at regular separations of 2.9 Å and a potential barrier of approximately 0.38 eV (Beyeler, 1976). In each crystal unit cell there are four channels in parallel, figure (2a), with a correlation length along the channels of approximately 35 Å, composed of channel unit cell groups of 3 to 6 minima each containing a vacancy, figure (2b), (Beyeler, 1976). Because of the strong ion-ion interaction the regularity of the spacing is distorted with an estimated displacement of about 22% neighbouring the vacancy. These supercell groups are combined together so as to satisfy the material stoichiometry, giving a gross structure which can only be described in terms of a probability distribution of supercell types. The similarity with the adsorbate system is now obvious, since the characteristic features of these are the presence of a sinusoidal surface potential, produced by the fixed structure of the surface, and a partial occupancy of the minima by the adsorbed species. Furthermore when the occupancy is of the order of 0.5 it would be reasonable to expect intermolecular interactions such as hydrogen-bonding

to distort the local structure of the surface potential which, however, is sufficiently strong to impose a near regular molecular ordering.

When we examine the other materials that exhibit the anomalous type of behaviour it is found that they fit into the same pattern of system. The ionic glasses are heterogeneous materials with crystallites providing an interior surface to the amorphous regions, whereas the stearic acid films are surface adsorbed via the organic acid ($-\text{CO}_2\text{H}$) groups which are likely to have a partial occupancy, particularly if charge injection from the electrode ionise some of the groups.

3. The Mechanism of Low Frequency Dispersion

In the preceding section we have identified the low frequency dispersion response with systems in which a mechanically rigid lattice forms a regular array of binding sites for ions or molecules, most of which are occupied. This large occupancy factor allows the bound species to interact with one another so as to modify the regularity of the inter-site spacing from that of the substrate potential. As a result the translational reproducibility will be destroyed over a distance ξ_c which defines a positional correlation length for the cluster of ions or molecules thus formed. For separations less than ξ_c patterns of local ordering will exist, such as the supercell groups in the Hollandites. In the water adsorbate systems it is likely that the local ordering is that of hydrogen bonding molecule groups whose network regularity is over-ridden at ξ_c by the greater spacing of the adsorbate sites.

If substrate systems such as these were sparsely occupied by a low concentration of ions charge transport could occur by particle hopping. Since each ion would have unrestricted access to an unoccupied site on a path connecting the electrodes a D.C. conductivity would be expected from them. When the site occupancy is high, however, access to sites on an electrode connecting pathway is substantially reduced when the dimensionality of the system is low. As a result charge transport in the highly occupied, low dimensionality, systems must be considered in an entirely different manner to that of the unrestricted hopping systems. The approach adopted here is a modification of that previously used to describe relaxation in condensed matter (Dissado and Hill, 1979, 1980, 1981; Dissado, 1982).

In this picture materials exhibiting relaxation phenomena are envisaged as being composed of clusters in which the perfect lattice structure is distorted. A macroscopic sample of the material will be formed with a steady-state distribution of such clusters varying continuously in form from complete distortion to a perfect lattice structure. This distribution should be viewed in the dynamic sense in which a particular cluster if labelled would be seen to adopt all the possible structures with a fixed probability density over a suitable time scale. This description should not be confused with that of a static distribution in which the structure would vary from site to site but remain constant in time. The mechanism whereby individual clusters fluctuate their structure is via inter-cluster (I-C) exchanges, which include the transport of distortion or strain by way of a virtual phonon process (Joffrin and Levelut, 1975) in addition to any particle exchanges that may be possible.

The response of such systems to an externally applied spatially uniform field is determined by the relaxation of the spatially uniform polarisation fluctuations (Kubo, 1957). This relaxation is a composite process in which

the evolution of the cluster structure from the spatially uniform displacement is initially dominant, to be followed at longer times by the evolution of the steady state cluster distribution (Dissado, 1982).

We have previously considered the situation in which the I-C exchanges do not themselves constitute a linear response of the applied field. As a result they act not as a noise (polarisation fluctuation) on the material polarisation but as a noise on the relaxation current of the polarisation (Hill et.al., 1981), retarding the approach to the dynamic equilibrium and thereby producing the observed loss peak response (Jonscher et.al., 1980; Dissado, 1982). However when the I-C exchanges carry a charge such as in the systems considered here they constitute an element of electrical current which couples linearly with the applied field. It is this difference which is the essential characteristic of the anomalous low frequency dispersion response which is observed.

3.1 Inter-cluster exchanges and the effective transport of charge

Because of the cluster nature of these systems the effective hopping of an ion between available sites will have a different effect depending on whether the distance covered, L , is less than or greater than the cluster correlation length ξ_c . When L is less than ξ_c the ion will still be partially correlated with its original site containing the counter charge and these processes must be regarded as polarising the cluster. Only when L is greater than ξ_c do the ion and counter charge reside in different clusters and move independently of each other. This process, which corresponds to cluster ionisation, generates in addition a new internal structure for the clusters evolved. In the Hollandites, for example, the supercell composition of the clusters will be different immediately following the interchange although an internal readjustment of the clusters to the presence of a hole or an extra ion will result from the ion-ion interactions. In its absence the inter-cluster exchange process constitutes an electrical current element which simultaneously creates a range of different cluster structures. Therefore a description of the evolution of the probability density of cluster structures will also give the distribution of the current elements produced by the charge carrying I-C exchange processes. This is achieved by determining the probability of realisation of a prepared initial state of the system at a subsequent time and convoluting it with the probability of realisation of a new state of the system (Hill et.al., 1981; Dissado, 1982).

The convolution is necessary because in a closed or conserved parameter system decay of the information placed in the initial description must inevitably mean the growth of that information in a redistributed form within the system, no mechanism being available to allow loss to an external sink. In this case the initial prepared state consists of a translationally equivalent set of identical neutral clusters whose internal structure satisfies stoichiometric requirements. The time development of the prepared state is determined by the inter-cluster exchange processes acting as a perturbation on the system. In the interaction representation the time development is given by

$$\psi(t) = \text{Real} (\exp[-i\bar{E}t] \exp\{ F(t) \}) \quad (4)$$

where \bar{E} is the average energy required to create the prepared state structure from the steady state equilibrium, and $F(t)$ describes the effect of inter-cluster exchange perturbations $V(t)$ in terms of their cumulants (Kubo, 1962; Chester, 1963)

(6)

$$F(t) = \sum_{q=1}^{\infty} (-i)^q \int_0^t dt_1 \int_0^{t_1} dt_2 \dots \int_0^{t_{q-1}} dt_q \langle V(t_1) \dots V(t_q) \rangle_c \quad (5)$$

The first non-zero contribution, $q = 2$, has the form

$$- \sum_{I,II} \frac{V_{I,II}^* V_{II,I} [1 - \exp\{-i(E_I - E_{II})t\}]}{(E_I - E_{II})^2} \quad (6)$$

which can be converted into the integral

$$\int_0^{\hbar\eta} N(E) \{1 - e^{-iEt}\} dE \quad (7)$$

where $E = E_I - E_{II}$ and $N(E)$ is the density of energy changes $\hbar E$ produced by the perturbation. The form of $N(E)$ is particularly important in determining $F(t)$ and can be deduced in the present case by considering the possible ways in which a given amount of energy can be utilised in producing inter-cluster exchanges.

The transport of charge between clusters, defined as an I-C exchange, possesses a number of possibilities in addition to the direct hopping of an ion between the respective clusters. There will be a continuum of these ancillary processes in which correlated I-C exchanges over shorter distances combine to give an effective charge transport over a long range. The number of such I-C exchanges required to produce an equivalent transport of charge will increase as their transfer range decreases, figure 3(a). Since the energy required to separate a charge from its counter charge increases with separation the number density $N(E)$ of inter-cluster exchanges at a particular energy E will increase as E decreases and the leading term in $N(E)$ will have the form

$$N(E) = p/E \quad (8)$$

which leads to an infra-red divergent behaviour (Hopfield, 1970) for $F(t)$

$$F(t) = ip\eta t - p\{E_1(\text{int}) + \ln(\text{int}) + \gamma\} \quad (9)$$

The average energy of excitations produced by the perturbation is thus

$$\hbar\langle E \rangle = \int_0^{\hbar\eta} \hbar E N(E) dE = p\hbar\eta \quad (10)$$

and since $\hbar\eta$ is the maximum energy change produced by the perturbation, that is the cluster ionisation energy, the index p must be unity or less.

Each of the I-C exchanges allowed for in $F(t)$ alters the internal structure of the clusters involved and thus the factor $\exp\{F(t)\}$ in equation (4) describes the development of the distribution of cluster structures as a self-energy clothing the prepared state. Because the prepared state requires the input of the average energy $\hbar\langle E \rangle$ in order to create it from the distribution it is this energy that is available through the perturbations $V(t)$ for the I-C exchanges creating the new structure and transferring the charges, hence

$$\hbar\bar{E} = \hbar\langle E \rangle = p\hbar\eta \quad (11)$$

The energy stored in the ordered cluster will be present as delocalised vibrations whose quanta are in excess of the localised vibrations of the disordered cluster. An alternative view of the evolution can be given in terms of the required changes in the vibrational quanta (Dissado, 1982).

The function $\psi(t)$ should be regarded in the quantum mechanical sense as the probability of realisation of the prepared state at time t , and is presented in its entirety in figure 4. This function approaches zero time as a gaussian with time reversal symmetry but when $nt \sim 1$ partial recurrence cycles set in as energy is exchanged between the prepared state and the I-C exchange fluctuations. At times in excess of nt being unity a power law decay dominates as the large number of different I-C exchange processes involved in the self-energy overdamp the prepared state irreversibly and clothe it,

$$\psi(t) \sim \exp\{-(nt/2)^2\} \quad ; \quad nt < 1 \quad (12a)$$

$$\sim (nt)^{-p} \quad ; \quad nt > 1 \quad (12b)$$

It should be noted that the long time decay of equation (12b) has been obtained without the aid of an arbitrarily introduced decay factor in the correlations of $V(t)$ contributing to $F(t)$ as is usual (Resibois and De-Leener, 1966) in problems concerning conservative systems. The long time development of $\psi(t)$ in equation (12b) shows that the probability of finding the prepared state at a time t decays as the alterations in cluster structure brought about by I-C exchanges grow. The probability of realising a clothed state at time t after it has started to form must therefore take the form

$$\bar{\psi}(t) \sim (\bar{nt})^p \quad ; \quad \bar{nt} > 1 \quad (13)$$

The probability density of cluster structures observed at time t can be obtained from the contributions of each I-C exchange event which occur with equal facility in each identical time interval. The contribution from an I-C exchange occurring at time t_1 is given by the probability of realising the new state at a time $(t - t_1)$ later weighted by the probability of finding the prepared state at time t_1 . This contribution is thus

$$P(t, t_1) = t_1^{-p} (t - t_1)^{+p} \quad (14)$$

and the average structure is therefore

$$\sum_{t_1} P(t, t_1) / \text{Number of elements} \rightarrow t^{-1} \int_0^t t_1^{-p} (t - t_1)^{+p} dt_1 \quad (15)$$

as the number of elements is proportional to t .

The establishment of the steady state distribution is presented schematically in figure 5, with a selected number of contributions shown. The probability density of cluster structures can be derived from equation (15) (Hill et.al., 1981) and is shown in figure 6 for a range of values of the index p . Although $P(t, t_1)$ only allows for single I-C exchange events the probability distribution obtained has been shown to be persistent when multiple events are included (Hill et.al., 1981) and thus represents a steady state description of the system.

The fluctuations producing the steady state distribution are driven by exchanges in stored energy between the competing features determining the short range and long range structure respectively. In the case of the Hollandites these are the intra-cluster ion-ion repulsions and the nett attraction between charged clusters. The resulting probability density therefore determines the configuration entropy of the inter-cluster super-structure and the inter-cluster exchanges produce fluctuations in the inter-cluster configuration entropy. Because a configurational entropy contribution to the probability of realisation is temperature independent for a given

state of the system the index p resulting from its fluctuations will also be temperature independent.

It is the special feature of the systems examined here that the I-C exchange processes transport an effective electrical charge and therefore constitute an elemental electric current. Each contribution $P(t, t_1)$ therefore represents a current element in the complete distribution as observed at time t . This observed current can therefore be obtained by averaging over the normalised cluster distribution

$$\langle J \rangle = [\Gamma(1+p) \Gamma(1-p)t]^{-1} \int_0^t j t_1^{-p} (t - t_1)^{+p} dt_1 = j \quad (16)$$

where j is the current element which is given by the rate of transport of the effective cluster charge over the correlation distance ξ_c . This expression can be best understood if each contribution $P(t, t_1)$ is taken to represent a number of sequential nearest neighbour cluster transports of effective charge in the time range $(t - t_1)$, the nett transport must then be divided by the number of primitive transports in time t , to give the average current.

3.2 The internal relaxation of clusters

The average current $\langle J \rangle$ given by equation (16) has the form of a D.C. current with fluctuations which give rise to power law noise (Hill et.al., 1981) which originates in the reorganisation of long range inter-cluster structure. In deriving this expression we have, however, neglected the possibility of recombination of the effective charge and counter charge. Since recombination can only take place for separations less than the cluster correlation length ξ_c the dynamics of this process are identical to the relaxation of a polarised cluster.

The time development of the relaxation function of a polarised cluster, $\phi(t)$ has already been obtained (Dissado and Hill, 1979; Dissado, 1982) as

$$\phi(t) \sim (\zeta t)^{-n} \exp\{-\omega_c t\} \quad (17)$$

which can be thought of as the possibility of realising the initial polarised state at a time t after relaxation has been initiated. Here ω_c is the relaxation rate of the cluster dipole rather than a site dipole and the $(\zeta t)^{-n}$ factor results from the evolution of the initial state into the distorted array that comprises the cluster structure.

In the system considered here each ion within a neutral cluster can be considered to form a site dipole with its lattice counter charge. The polarisation fluctuation coupled to the spatially uniform applied field consists of completely in-phase displacements of the site dipoles along the direction of the field. This is equivalent to the displacement of an effective cluster charge over a distance ξ_c , figure 3(b), just as the I-C exchanges are equivalent to an effective displacement of this cluster charge over macroscopic distances.

The spatially uniform fluctuation can be considered to be a prepared state of the cluster which will decay into the distorted structures available. This behaviour can be described as in the previous section by considering the initial state to be created from the average steady state cluster structure with an amount of energy kT stored in the structural ordering. This energy is available through perturbations $V(t)$ to reorganise the cluster structure into the available distorted forms. As previously there will be an increasing number of ion displacement processes as the energy requirement for the individual process becomes less. This will lead to an infra-red divergence as previously

discussed and give the time power law decay, $(\zeta t)^{-n}$, of the initial state found in equation (17). Here the average energy of fluctuation formation is

$$\bar{n} \bar{E} = n \bar{h} \zeta \quad \text{with } 0 \leq n \leq 1 \quad (18)$$

and ζ is the maximum energy change required by a single cluster distorting process. In the present case ζ is the energy change introduced when an ion is moved into a neighbouring vacancy with all the other cluster ions undisplaced and it may involve details of the local potential surface as well as ion-ion repulsions. The processes involved in the t^{-n} decay are those establishing the steady state configurational entropy density of neutral cluster structures and thus we may expect n to be also temperature independent unless a structural ordering process is taking place in the local order. In general n is expected to be different in magnitude from p since n is related to the local structural order, whereas p is related to the long range inter-cluster order.

The exponential decay factor of equation (17) originates from the cluster-dipole relaxation process in which all memory of the initial prepared state is lost. These are processes that involve an external energy system such as a thermal bath and are describable by a deterministic rate equation where ω is the cluster relaxation rate. In pseudo one-dimensional systems such as the Hollandites the cluster relaxation rate is identical to the recombination rate for the effective cluster charges, however in two-dimensional systems, such as those of the water adsorbates, additional routes may be available for the cluster dipole relaxation which do not involve recombination. The time scale for the relaxation of the cluster is then not the same as the time scale for the onset of the inter-cluster exchange processes.

3.3 The composite process.

In the preceding sections the presence of clustering in the systems described has forced the ion transport processes to be divided into intra- and inter-cluster motions with distinctly different effects. When considering the response of these systems these two types of motions have to be combined into a composite process.

Since we are interested in the response to a spatially uniform field it is necessary to consider the time development of an initial (prepared) state with spatially uniform polarisation, figure 3(c). The total polarisation of this state is identical to that given by the separation of the effective cluster charge, δ , over macroscopic distances and these therefore represent equivalent descriptions of the total polarisation of the system by an applied field.

Inter-cluster exchanges will transport the effective charge through the system as described in section 3.1 such that $(\eta t_1)^{-p}$ represents the probability that an effective charge is untransported at time t_1 and $\{\eta(t - t_1)\}^p$ represents the probability that an effective charge available at time t_1 has been transported at time t .

The effective cluster charge can take part in inter-cluster exchange processes as a charged entity because its separation from the counter charge, ξ_c , is the cross-over length between motion as an independent charge and as a bound cluster dipole. The recombination of effective charges, cluster relaxation, will act as a competitive process to the inter-cluster exchange transport and thus the probability of finding a unit charge available for

(10)

transport at time t_1 will be

$$\exp\{-\omega_c t_1\} (\zeta t_1)^{-n} (nt_1)^{-p} \quad (19)$$

and the contribution of an inter-cluster exchange initiated at time t_1 to the current observed at time t is

$$j_0 \exp\{-\omega_c t_1\} (\zeta t_1)^{-n} (nt_1)^{-p} [\eta(t - t_1)]^{+p} \quad (20)$$

where j_0 is the bare current element for nearest neighbour site ion hopping unperturbed by the internal structure of the cluster (Dissado and Hill, 1980). The current observed at time t is the average of the contributions represented by equation (20), and is thus

$$\langle J(t) \rangle = \frac{j_0 (\zeta/\omega_c)^{-n}}{\Gamma(1+p) \Gamma(1-p)} \int_0^t e^{-\omega_c t_1} (\omega_c t_1)^{-n} t_1^{-p} (t-t_1)^{+p} dt_1 \quad (21)$$

where $\Gamma(1+p) \Gamma(1-p)$ is the normalisation factor of the distribution, figure 6, and

$$j_0 (\zeta/\omega_c)^{-n} = j_c \quad (22)$$

is the clothed (renormalised) cluster current. Carrying out the integral gives

$$\langle J(t) \rangle = j_c e^{-\omega_c t} (\omega_c t)^{-n} {}_1F_1(1+p; 2-n; \omega_c t) \frac{\Gamma(1-p-n)}{\Gamma(2-n) \Gamma(1-p)} \quad (23)$$

where $\Gamma(\)$ is the gamma function and ${}_1F_1(\ ; \ ;)$ the confluent hypergeometric function (Slater, 1960).

The complex dielectric susceptibility is given by the one-sided fourier transform of $\langle J(t) \rangle$ as

$$\chi(\omega) = j_c \frac{N d_c}{\omega_c kT} \frac{\Gamma(1-p-n)}{(1-n) \Gamma(1-p)} F(\omega/\omega_c) \quad (24)$$

in which $d_c (=e\xi_c)$ is the unperturbed cluster dipole strength, N the number density of clusters and $F(\omega/\omega_c)$ the dielectric shape function as a function of frequency scaled to the cluster relaxation rate which is given by

$$F(\omega/\omega_c) = \left(\frac{\omega_c}{\omega_c + i\omega} \right)^{1-n} {}_2F_1(1-n, 1+p; 2-n; \frac{\omega_c}{\omega_c + i\omega}) \quad (25)$$

in which ${}_2F_1(\ , \ ; \ ;)$ is the gaussian hypergeometric function (Slater, 1966).

The dielectric function contained in equation (24) adequately describes the response observed in materials exhibiting the anomalous low frequency dispersion behaviour as can be seen in figures 7 and 8 where it is applied to results obtained for Hollandite, humid sand and a heterogeneous ionic glass. The asymptotic forms of $F(\omega/\omega_c)$ at high and low frequencies, with respect to ω_c give

$$\chi'(\omega) \approx \chi''(\omega) \approx \chi'(\omega_c) (\omega/\omega_c)^{-p} ; \quad \omega < \omega_c \quad (26a)$$

$$\chi'(\omega) \approx \chi''(\omega) \approx \chi'(\omega_c) (\omega/\omega_c)^{n-1} ; \quad \omega > \omega_c \quad (26b)$$

where the factor $\chi'(\omega_c)$ is given by

$$\chi'(\omega_c) = \frac{j_c N_c d_c}{\omega_c kT} \quad (27)$$

with T the temperature and k Boltzmann's constant.

Kramers-Kronig relationships are obeyed throughout and in both the asymptotic regions relationship (2) is obeyed, a result which allows the indexes p and n to be deduced experimentally with some accuracy however closely they approach either unity or zero. The frequency ω_c determines the cross-over from high to low frequency behaviour and no semblance of a loss peak is observable in $\chi''(\omega)$ although a small plateau can occur in $\chi'(\omega)$ for large values of p and smaller values of n . This means that a loss peak arising from short range hopping does not occur in these materials although such a loss peak has been expected (Pollak and Geballe, 1961), since the site dipole hopping processes combine to produce a whole cluster relaxation which goes over continuously to the longer range inter-cluster exchange transport at the frequency at which the loss peak would be expected.

The amplitude of the response $\{\chi'(\omega)\}$ at the cross-over frequency ω_c simultaneously represents a continuous cross-over between the dipole strength arising from a cluster polarisation of length ξ_c and effective dipoles arising from transport of the effective cluster charge over inter-cluster distances.

For these reasons both regimes of the anomalous low frequency dispersion must be regarded as a single distinct loss feature whose properties are scaled to that of a cluster such as its length, ξ_c , polarisation and recombination/relaxation rate ω_c . Only if the cluster possesses additional routes for polarisation relaxation which do not involve recombination will a separate loss peak be resolvable, which nonetheless will also form part of the composite system (Eden et.al., 1980)

3.4 The relationship of anomalous low frequency dispersion and the indices p and n to material structure.

The theoretical description in the previous sections has shown that anomalous low frequency dispersion is a response resulting from the relaxation of a spatially uniform displacement of charge in a system with a spatially disordered partial occupancy of ion binding sites. Initially, for $\tau < t < \tau_c$, the spatially uniform displacement over macroscopic distances evolves into identical displacements correlated over the cluster size ξ_c . For times $t > \tau_c$ exchanges of ions between clusters transports an effective charge to the boundaries of the system and alters the internal structure of the intervening clusters thereby producing a steady state distribution of their structures.

i) The index n

This index has previously been identified (Dissado and Hill, 1979) as the dynamic correlation index for the intra-cluster displacement motions, it therefore measures the efficiency with which displacements are transmitted within the cluster. An alternative definition of n is obtained from the average energy required to establish the prepared state of spatially uniform displacement, as a fraction of the maximum possible energy required to establish this state,

$$n = \bar{E}/\zeta \quad (28)$$

$n\zeta$ is also equivalent to the maximum binding energy of the cluster when it is created from the prepared state with \bar{E} the average binding energy (Dissado, 1982; Hill and Jonscher, 1982). In these terms small values of n ($\rightarrow 0$)

correspond to a weak distortion of the spatially uniform initial state and hence a highly irregular cluster of distortion such as might result from an interstitial ion. Large values of n ($\rightarrow 1$) correspond to clusters that strongly distort the spatially uniform initial state and are tightly bound. Such clusters will have a highly regular internal structure which is nearly dissociated from the regularity of the host lattice or matrix from which they are created. A value of n identical to unity would be impossible since it would correspond to clusters which are completely divorced from their environment.

The Hollandites typically have values of n in the range 0.6 to 0.8, which shows that the ion-ion repulsions which cause the clustering substantially override the regularity of the binding site array (Beyeler, 1976). A value of n of 0.8 however although high is by no means as high as some that have been observed in loss peak processes (Hill, 1981a; Shablakh et.al., 1982a & b) where steric and topographical features almost isolate one crystalline domain from another.

ii) The index p

This index has been identified with the dynamic correlation index for inter-cluster exchange processes (Dissado and Hill, 1979). Therefore in these systems p indexes the efficiency of transport of the cluster effective charge. An alternative definition of p also exists in terms of the average energy given up by the system when the prepared state is converted to the steady state equilibrium through inter-cluster exchange processes as a fraction of the maximum energy available

$$p = \bar{E}/\eta \quad (29)$$

The probability density of cluster structures, figure 6, shows that when p is small and approaches zero the clusters' structures remain almost identical as in the prepared state and the distribution is almost a delta function. When p is large ($\rightarrow 1$) the range of cluster structures is wide and essentially unbounded. Thus as p approaches unity the inter-cluster exchange fluctuations carry the change of cluster structure far away from their origin. In the systems showing a low frequency dispersion the inter-cluster exchange processes transport an effective charge, hence as p approaches unity the effective charge is transmitted so as to affect very many clusters. In the limit of p becoming unity the transported effective charge affects all clusters and the distribution becomes unbounded.

The same understanding of p can be obtained if section 3.1 is followed in regarding \bar{E} as the energy stored in the structural fluctuation defined as the prepared state. This energy is available through inter-cluster exchange processes to transport an effective charge. The maximum energy required by inter-cluster exchanges, $\eta\eta$, is that required to transport the effective charge to the sample surface and p is the fraction of this that is available from the structural fluctuation. A value of p identical to unity would correspond to a situation in which sufficient energy existed in structural fluctuations to completely remove the effective charge from the sample. The range of transport involved would be infinity and result in a normalisation factor of infinity in equation (16). Because an effective charge is ejected this value is impossible to realise unless the cluster reduces to a single ion, in which case a D. C. current ensues.

The values of p typically observed in low frequency dispersion lie between 0.7 and 0.99 and correspond to systems which approach perfect transport. The long range structural description of such systems is one of a wide

distribution of types of cluster structures with the average cluster structure described by the index n . For example in the Hollandites we may expect to find a range of differing clusters corresponding to the number of ways of combining the different supercell elements within the cluster correlation length. This type of structure could be expected to occur whenever there exists a number of local structural elements whose size is incompatible with the cluster correlation length which will be determined by the interactions between the elements arising from their assembly. This description could be expected to be appropriate to the types of systems known to exhibit the anomalous low frequency dispersion response.

3.5 Hydrogen-bonding systems

In the preceding sections pseudo one-dimensional ionic systems such as the Hollandites have been mainly used as examples of low frequency dispersion. A two-dimensional network of hydrogen bonded molecules however constitutes a second class of materials which exhibit this type of response, often with some special features of their own. In these systems clustering will occur because hydrogen-bonding will over-ride the binding site array structure on a local scale. The proton in the H-bond performs the function of the ion in the Hollandites and the cluster will be polarised by a succession of transfers in the H-bonded system leaving a hydrogen bonded $-OH$ group at the end of one path and a hydrogen bonded $-OH_2$ at the other. As with the Hollandites there will be a number of paths such that the number of transfers increases as the individual charge separation energy decreases. In a similar manner effective proton transfer over distances greater than the cluster correlation length will generate inter-cluster exchange processes. Because only nearest neighbour proton hops are allowed, direct proton transfer being inoperative except as a thermally activated mechanism in a completely connected system (Freund, 1981), a two-dimensional spatiality is necessary to give the limited number of alternative routes required for the power law 'evolution' mechanism.

The intra-cluster regularity of these systems can be expected to be less than that in Hollandites because of the presence of weak as well as strong bonds and this is reflected in the much lower value of n that is often observed, typically of the order of one half. Since the molecular structure can be expected to distort somewhat to accommodate the incompatibility of the short range H-bonding and long range site structure the index p should be slightly less than those observed in the Hollandites and is typically of the order of 0.8 to 0.9.

The main difference that can be observed in these systems is the presence of a subsidiary loss peak, as shown in figure 9, which cannot be separated from the onset of the low frequency dispersion even although the loss peak frequency can be shifted through several orders of magnitude by variation of one of the several parameters such as temperature or humidity. This behaviour occurs because the two-dimensional system has additional routes for relaxation which do not involve charge recombination. In this case the characteristic frequency for the anomalous dispersion, ω_c , is less than that of the loss peak, ω_p , and the cluster dipole has relaxed even although the effective charge is still available to take part in the inter-cluster exchanges. The response can therefore be regarded as the sum of separate low frequency dispersion and loss peak processes, however in these systems one further feature leaves them coupled, the temperature dependence of ω_p and ω_c is identical. This can be understood if the recombination is regarded as a direct intra-cluster transfer of a proton by activation over a H-bond potential barrier

with the pre-exponential factor a proton vibration frequency multiplied by an attempt factor giving the total number of different routes available for recombination (Hill and Dissado, 1982). The relaxation of the cluster dipole will also require an identical activation energy but will include routes by which the molecules are rotated following H-bond breaking which is later re-created. Since the rotation motions are coupled to the translation motions in a H-bond (Witkowski and Wojcik, 1973) the same activated state can be entered through either type of motion and the phonon frequency will be identical in ω_p and ω_c , but ω_p will contain the totality of routes whereas ω_c will only contain the fraction that leads to charge recombination, that is

$$\frac{\omega_c}{\omega_p} = \frac{\text{Number of routes giving recombination}}{\text{Total number of routes leading to relaxation}} \quad (30)$$

Under these circumstances a cluster loss peak is observed at ω_p whose high frequency tail (ω_p^{n-1}) contains the index n appropriate to the regularity of the site dipole structure which is also the intra-cluster regularity of the H-bond structure. On the low frequency side of the loss peak (ω_m) the inter-cluster exchange process starts to produce a distribution of cluster structures but does not yet lead to an effective transport of charge because the charges have not yet recombined in the polarised intermediary clusters along the transport path, figure 3. In this frequency region the inter-cluster exchange processes play the role previously assigned to them in loss peak processes (Dissado and Hill, 1979; Dissado, 1982). The loss peak index m will therefore have the same value as that of p in the low frequency dispersion observed at frequencies less than ω_c , as seen in figure 9. The effect of humidity also finds a simple explanation in these terms since adsorption of extra molecules will occur in the vicinity of the primary adsorption sites expanding the cluster and rapidly increasing the number of routes available for relaxation. The local structural order is determined by the short range H-bonding which is unaffected leaving n and the ratio of frequencies, equation (30), unchanged.

The relationship of the cluster relaxation process to the low frequency dispersion is illustrated in a sequence of results obtained from the cyclo-alcohols (Shablakh et.al., 1982b). In the plastic crystal phases of cyclopentanol and cyclohexanol hydrogen bonding over-rides the orientational ordering of the molecules and the clusters are combined into a three-dimensional network. Because of the three-dimensional spatiality a substantial number of fully connected routes will exist allowing an activated direct proton transport and D.C. characteristics. The larger number of cluster relaxation routes produces a separate relaxation peak, figure 10, whose temperature behaviour is the same as that of the D.C. conductivity. The inter-cluster exchange routes that are not involved in the D.C. conductivity act as structural fluctuations on the loss peak giving an index $m = 0.85$, their low frequency dispersion contribution being short circuited by the D.C. current. Following a time dependent transformation into an ordered crystal phase the three-dimensional network is disconnected and the remaining two-dimensional boundary regions now contribute an anomalous dispersion with a value of p identical to that of m for the plastic crystal. The values of n in the two states is also identical as can be seen in figure 11. A similar behaviour is observed in cyclohexanol where in the ordered crystal phase III the cluster loss peak is not quite resolved from the low frequency dispersion to which it retains its relationship over four decades of frequency change for ω_c , figure 12.

4. Limits of the Low Frequency Dispersion Response

The mechanism of low frequency dispersion described in the previous section relates the response to the inter-play between short range and long range motions which are scaled to the cluster size ξ_c . This result will clearly break down at very high frequencies when only the motions of ions which do not affect the environment will respond, and also at very low frequencies when the ions may break free from the inter-cluster exchange routes or the finite size of the sample have an effect. Each of these features defines a limiting behaviour which may be observed experimentally.

4.1 High frequency limit

For frequencies $\omega > \omega_c$ the response of the system is contributed by the individual processes generated by the perturbations $V^i(t)$ that reorganise the structural ordering of the prepared states. The low energy ($\hbar\omega$) motions are those in which individual site displacements occur in phase throughout the cluster. Their limiting intra-cluster energy is equivalent to the recombination frequency ω_c which thus defines a cut-off to the infra-red divergent behaviour as shown in equation (17). Higher frequencies which correspond to higher energy adjustments involve displacements whose phase can be defined by a wavevector q that progressively increases (Hohenberg and Halperin, 1977). At very high frequencies and wavevector only nearest neighbour motions are coupled together strongly. The effective charge will therefore vibrate as a site bound ion in the total cluster potential. Its vibrations will be equivalent to oscillations of the effective cluster dipole, figure 3(d), and their frequency ζ will be a measure of the binding energy of the cluster dipole as a correlated entity, that is the maximum cluster binding energy. This frequency will therefore represent the upper limit of the infra-red divergence and will produce the oscillations shown in figure 4 which become more pronounced as n approaches unity and the average cluster structure becomes more ordered giving more correlated motion.

The high frequency limit ζ therefore determines the cross-over from the power law ω^{n-1} response to a different type of behaviour. If we examine the susceptibility at this frequency we find that

$$\begin{aligned}\chi'(\omega=\zeta) &= \chi'(\omega_c) (\zeta/\omega_c)^{n-1} \\ &= (j_o/\omega_c) (N_c d_c) (\omega_c/\zeta) \\ &= j_o N_s d_s / (\zeta kT)\end{aligned}\quad (31)$$

where N_s is the number density of site dipoles d_s .

Expression (31) shows that ζ represents the cross-over from the infra-red divergent tail of a relaxation process to a resonant behaviour with j_o representing the rate of change of the site dipole and therefore incorporating the damping factor (ω) of the oscillations. More precise details of this frequency region are necessary if a complete description is required, however an echo of it appears in the coupling strength $\chi'(\omega_c)$ where the coupling strength of the high frequency process has been clothed to become

$$\chi'(\omega_c) = j_o (N_c d_c) (\zeta/\omega_c)^{n-1} (\omega_c kT)^{-1} \quad (32)$$

If we can take

$$j_o = d_c \omega_c = d_s \omega_s \quad (33)$$

as expected from the perfect correlation of figure 3(d), then

(16)

$$\chi'(\omega_c) = \frac{d_c^2 N_c}{kT} \left(\frac{\omega_c}{\zeta}\right)^n \quad (34)$$

and the factor $(\omega_c/\zeta)^n$ defines the reduction of the cluster charge to its effective value by the clothing.

4.2 Low frequency limit

(i) Sample size effect

For frequencies $\omega < \omega_c$ the anomalous low frequency dispersion (ω^{-p}) results from the response of the I-C exchange processes. As the frequency is reduced lower energy inter-cluster exchange processes which coherently transport a proportionally larger fraction of the effective cluster charge, equation (8), contribute to the response. A macroscopic dipole moment is produced across the sample thickness which increases as the frequency is lowered, ($\chi' \propto \omega^{-p}$). A limit to the polarisation will be reached for finite sized samples when the effective charge is completely transported to the boundaries thus defining the lowest frequency of the I-C exchange processes which will correspond to in-phase transport across the sample thickness D , with wavevector $q \sim D^{-1}$. The capacitance can be expected to saturate at this frequency, as observed in figure 13. At lower frequencies non-linear effects may occur (Garton, 1939) and a D.C. conductivity may arise if the presence of an effective charge allows the surface ions to be discharged.

(ii) Onset of particle diffusion

The presence of an effective charge transport by way of the low frequency dispersion mechanism relies on the restriction of ion or proton motions to their respective one or two-dimensional pathways along which structural readjustments can transport. When the ions or water molecules can be removed completely from the pathways they will become free to diffuse in the three-dimensional host matrix independently of the clusters which are confined to the paths. The mechanisms causing such scattering will need sufficient energy to remove an ion/molecule from its binding site and the cluster in addition to a change in momentum vector and can be composed of either activated phonon processes or scattering off topographical imperfections of the host matrix. A time t_d can therefore be defined as the lifetime with respect to these processes. At frequencies lower than $\omega_d \sim t_d^{-1}$ the response assumes the familiar three-dimensional diffusion form (Carslaw and Jaeger, 1959)

$$\chi'(\omega) \propto \chi''(\omega) \propto \omega^{-1/2} ; \quad \omega < \omega_d \quad (35)$$

The cross-over frequency will define a path length ξ_d for ion/molecule three-dimensional scattering and a cross-over of this form has been discussed (Shapiro and Abrahams, 1981) for the transport of electronic wavepackets. For the latter case ω_d has been estimated to be of the order of 10^{10} Hz or higher, a frequency where it would be difficult to observe the cross-over. In the ionic systems discussed here, however, it can be expected that the cross-over frequency would be much lower and in many materials such as the Hollandites with their weak interaction between channels it may not occur at all in the observable frequency range. It has however been observed in several systems including ionic glasses, pyridine (Shablakh et al., 1982a) and the organic membrane egg lecithin with cholesterol (Jonscher, 1978). The last of these examples is shown in figure 14 where the cross-over is shown in a striking fashion and the diagram reveals in addition that the temperature behaviour of ω_d is not related to that of ω_c . We may expect $\omega_d > \omega_c$ at high temperatures in this system when the clusters themselves would be dissociated by the free particle diffusion, perhaps indicating the onset of biological deterioration in this particular case.

The onset of particle diffusion carries the system into the classical macroscopic regime and although lower frequency processes may be observed they will not be discussed here.

5. The Relationship of Low Frequency Dispersion to Power Law Electrical Noise

Expression (24) for $\chi'(\omega)$ can be converted to an A.C. conductivity $\sigma(\omega)$ as, (Kubo, 1957),

$$\sigma(\omega) = \omega \chi''(\omega) \quad (36)$$

giving

$$\sigma(\omega) \approx \chi'(\omega_c) \omega_c^p \omega^{1-p} \approx \chi'(\omega_c) \omega_c^p \quad ; \quad \omega < \omega_c \quad (37a)$$

$$\text{and} \quad \sigma(\omega) \approx \chi'(\omega_c) \omega_c^{1-n} \omega^n \quad ; \quad \omega > \omega_c \quad (37b)$$

In materials exhibiting low frequency dispersion p is often very close to unity and hence $\sigma(\omega)$ in the region $\omega < \omega_c$ has often been assumed to be the D.C. conductivity, from which it is virtually indistinguishable as shown in figure 15. However a simultaneous measurement of $\chi'(\omega)$, which has the same frequency dependence as $\chi''(\omega)$, will reveal that this is not the case. The relationship between A.C. conductivity and D.C. conductivity described by Almond et.al. (1982) for Na β -alumina results from equation (37) with $p \approx 0.99$ and $\chi'(\omega_c)$ essentially independent of ω . This latter result, which is not of general applicability (Jonscher, 1978), has implications for the temperature dependence of ζ and j_0 in Na β -alumina and related materials.

That low frequency dispersion does not represent a D.C. conductivity can be seen from its derivation since the effective cluster charge that is transported decays via cluster relaxation and recombination giving an average current $\langle J(t) \rangle$ in equation (23) that clearly decays monotonically with time for $t > \omega_c^{-1}$, albeit extremely slowly, figure 16. The behaviour of $\langle J(t) \rangle$ gives a description of the processes involved in low frequency dispersion. Initially a steep decay ($\propto t^{-n}$) results as the site displacement of a unit charge is clothed by the cluster readjustments to give the nett displacement of an effective charge over the cluster length ξ_c . The effective charge will be smaller as the cluster binding energy increases resulting in a larger value of n which is necessary to achieve the larger reduction in current required over the cluster size. At times greater than $t \approx \omega_c^{-1}$, which is an intra-cluster transit time for the effective charge, inter-cluster exchanges transport the effective charge through the disordered array of clusters with an efficiency denoted by p , such that no further decrease of charge occurs when p is unity. The hypothetical case of $n = 0$ and $p = 1$ will therefore correspond to a perfect D.C. current.

When the electrodes to the system have such a nature that it is possible to exchange charge with the ionic system without deteriorating the electrodes or building up a neutral barrier a D.C. current will flow under constant operating conditions whose magnitude will be dependent upon the sample size since the t^{p-1} process will be cut-off at a time equivalent to the sample transit time for the effective charge. The processes giving rise to the low frequency dispersion will now be observed as a noise on the current. We have previously related expression (16) to power law noise in electrical systems (Hill et.al., 1981) with the result

$$\text{Noise Power} \propto (1/\omega)^\alpha \quad ; \quad \alpha = 2(1-p) \quad (38)$$

The present description of low frequency dispersion shows that the noise arises from structural order fluctuations in the disordered array of clusters by means

of which an effective charge is transported as a current. Energy is lost irreversibly when these fluctuations drive the thermal processes involved in intra-cluster relaxation as can be seen from the decay of response current $\langle J(t) \rangle$, as shown in figure 16. Thus intra-cluster relaxation also contributes a thermal noise to the system.

The power index, α , of the power law noise is dependent upon p , such that white noise results if p is unity and the correlation of transport processes perfect. This corresponds to an unbounded steady state distribution of cluster structures. When p is zero the cluster distribution is a delta function corresponding to a superlattice of identical clusters and the noise becomes gaussian ($\propto \omega^{-2}$). The distinction between these two limits lies in the number of random inter-cluster exchange events in a fixed time interval (Feynman and Hibbs, 1965) given by the normalisation factor of equation (16) which is infinite for the unbounded distribution producing the white noise and unity for the superlattice which exhibits gaussian noise.

These limits are unachievable in practice for the systems considered here and values of α in the range from about 0.4 to zero are to be expected. When the classical diffusion process occurs we may consider p to be 0.5, in which case α is unity and the noise becomes inversely proportional to the frequency. In electronic systems in which the diffusion process starts at very short times ($< 10^{-10}$ to 10^{-13} s) it will be this process that will be commonly observed, whereas in systems such as polymers we may expect values significantly different from unity (Pender and Wintle, 1979).

It should be noted that a normal D.C. response, equation (3), will be obtained for systems possessing electrodes that pass a current, the anomalous low frequency response only being observed when the electrodes block the passage of a current, or the system is confined to structural domains which are not connected to the sample electrodes.

6. Relationships to Other Models

The description of the low frequency dispersion mechanism presented here relates the response to the detail of the material structural ordering on a size scale which links the microscopic motions of the local structure with the near macroscopic behaviour of the whole structure. The technique adopted to achieve this result is in the spirit of the path integral formalism (Feynman and Hibbs, 1965). A specified fluctuation of the structural order is prepared as a wavepacket of the weighted microscopic disordering process and allowed to evolve. In this manner dynamic indices determining the evolution can be related to the degree of structural change arising in re-creating the disordered steady state equilibrium state from the prepared state.

This method is by its nature semi-microscopic and semi-stochastic and hence wide ranging. Several models however have been proposed for this and related phenomena which cover some of the features described here but are insufficiently comprehensive to describe them all. These will be briefly described so that their relationship to the present work can be made explicit and their differences, if any, outlined.

6.1 Jonscher's screened hopping model

In this approach it was suggested (Jonscher, 1975) that subsequent to a hopping transport a charge carrier was screened by its environment reducing

the charge to a factor f of its original value. As a result elementary considerations of stored and dissipated energy gives

$$\cot(n\pi/2) = \frac{\chi''(\omega)}{\epsilon'(\omega) - \epsilon(\infty)} = (1 - f)/f \quad (39)$$

In this model the intra-cluster region of response corresponds to the motion of weakly screened charges ($f \rightarrow 1$), which store a large fraction of the electrical energy in a recoverable manner. This description is equivalent to that of a cluster whose binding energy and internal correlation of motions allows it to store a large proportion of energy in the relative motions of ions. However because the ions are not screened from each other these motions are strongly coupled within the cluster, as recognised by Beyeler (1976) and not weakly interacting as suggested by Jonscher. The weakness of the screening in his model arises from the poor binding to the counter-ion potential within the cluster.

If we denote p as $1 - n'$ Jonscher's model is again physically accurate in describing the inter-cluster exchange regime as arising from the transport of strongly screened charges. The weakness of the original argument lies in its divorce from the detail of material structure. This was partly remedied by Ngai et.al. (1979) who attributed the power law response to excitations of states characterising the correlations of the particles. No attempt was made, however, to relate this behaviour to a detailed structure. There is, in fact, a considerable difference of interpretation between Ngai's model and the approach described here and elsewhere (Dissado, 1982) since in the latter the energy changes occur as alterations in the local vibrational frequencies as an ordered structure evolves to a disordered one via correlated site displacements rather than the excitation of a sub-system of states. An additional feature is the conservation of total energy between the forces favouring ordering and those which disorder. Ngai's suggestion that the low frequency dispersion involved two totally independent processes, the lower frequency behaviour dominating because of a stronger coupling constant, also cannot be upheld in the light of the experimental evidence of such features as diffusion. As a consequence the relationship between the intra and inter-cluster regimes was not recognised.

6.2 Cluster self-energy

In several problems concerning a region of structural order the static and dynamic response can be related to the self-energy of the structurally ordered cluster, giving (Hohenberg and Halperin, 1977)

$$[\chi(q=0, \omega)]^{-1} = [\chi_0(q=0, \omega)]^{-1} + \Sigma(q=0, \omega) \quad (40)$$

where χ_0 is the unclothed susceptibility and Σ the self-energy. In problems involving a non-conserved property such as is the case following the introduction of relaxation into the low frequency dispersion mechanism the self-energy has a logarithmic divergence

$$\Sigma(q=0, \omega) \approx \ln \omega \quad (41)$$

and self-consistent solutions are sought by way of a renormalisation group technique or exponentiation (Hohenberg et.al., 1972) leading to a power law dependence of the clothed susceptibility

$$\chi'(q=0, \omega) \propto \chi''(q=0, \omega) \propto \omega^{n-1} \quad (42)$$

This behaviour is identical with that of equation (26) which results from a method that assumes exponentiation in that the influence of higher order cumulants in equation (5) are neglected and treats the problem in the time

rather than in the frequency domain.

The self-energy in equation (40) results from a model of the static cluster response in which the possible cluster displacements are averaged over the cluster sites to give a site probability density of displacement (Kogut and Wilson, 1972) which is non-gaussian. Values of n approaching unity as appropriate to the intra-cluster structure are equivalent to a well ordered, highly correlated, structure. When p approaches unity ($n' \rightarrow 0$) the structural order is very weak corresponding to the inter-cluster ordering.

It is interesting that the often used modulus representation of dielectric permittivity (cf. Wong and Angell, 1976) presents the experimental results in the form of equation (40). In the low frequency region, it is shown in the modulus plot of figure 17, that

$$\text{Real} \left[\chi(q=0, \omega) \right]^{-1} \rightarrow 0 \quad (43)$$

as $\omega \rightarrow 0$ and thus the effective charges in the intra-cluster exchange regime are highly screened from each other as we have determined. The modulus, or inverse complex susceptibility, has the interesting feature that the plot of low frequency dispersion data yields a peak in the imaginary component making determination of ω_c relatively easy.

6.3 Scaling approach

The scaling technique has been used extensively to describe systems in which order exists only over a finite sub-macroscopic size. Basically the aim is to determine the extensive property $P\{L\}$ of a system as a function of its size. Starting from a small sized element for which a nearly exact calculation can be made, the size is increased by a constant factor b and the property $P\{bL\}$ recalculated. When the smaller system has the same functional dependence on size as the larger the original element can be seen to be a smaller sample of the larger system with the same intensive properties. The fundamental hypothesis of the technique, which was suggested by Kadanoff (1966), is that a minimum element of structure exists whose form is retained as the size scale increases. This assumption leads to the relationship

$$P\{bL\} = f(b, P\{L\}) \quad (44)$$

which has been applied by Abrahams et.al. (1980) to the analysis of the static electronic conductivity of disordered systems. The size dependence of the required property can be determined from equation (44) by dimensional arguments only if the system is perfectly ordered, any disorder contributes an infra-red divergent self-energy which leads to an anomalous dimensionality (Wilson and Kogut, 1974; Abrahams et.al., 1980). This index determines the structural relationship of the scaled-up element to its precursor and is directly related to the dynamic index n (Hohenberg and Halperin, 1977) which therefore describes the structural regularity in this sense. It should be regarded as a necessary factor in the description of structural ordering in addition to a correlation length.

When the method is applied to the present problem the static susceptibility is first determined as a function of the length L . Determination of the eigenfrequency $\omega(L)$ for a fluctuation of the same length then enables the dynamic susceptibility to be obtained (Shapiro and Abrahams, 1981) as a function of frequency. The field is considered to couple individually to the fluctuation with the static susceptibility for a given length over a continuum of lengths up to the sample size D . If, for example,

$$\chi(L) \sim L^x \quad \text{and} \quad \omega(L) \sim L^{-y} \quad (45)$$

$$\text{then} \quad \chi(\omega) \sim \omega^{n-1} \quad \text{with} \quad n = 1 - x/y \quad (46)$$

Previous work has been concerned with the transport of an electron wave packet (Thouless, 1973; Shapiro and Abrahams, 1981) and not with wave packet formation which would be equivalent to the intra-cluster processes considered here. The cluster, however, can be scaled in the same way with the minimum structural element being the site dipole. The observation of a value of n approaching unity for a frequency range of several decades shows that the susceptibility, and thus the polarisation of the fluctuation, is only weakly increasing with fluctuation size within the cluster, while the frequency is strongly size dependent. The polarisation coupling to a uniform field is that of an in-phase displacement and will be independent of the cluster size if the site displacements are fully correlated as independent Fourier components. When the site displacements have zero correlation the polarisation will be proportional to the cluster size. All real systems will lie between these two extremes with n approaching unity corresponding to strong correlation as concluded in section 3.

The wave-packet transport behaviour is equivalent to the inter-cluster exchange regime, and the value of $p \rightarrow 1$ observed over a large frequency range indicates a strong length dependent increase of the polarisation and hence a nearly uncorrelated inter-cluster structure. It follows that the current appropriate to this regime will consequently show a weak decrease with length giving a conductivity dependent upon the sample size as long as the low spatial dimensionality ($d \leq 2$) is retained (Abrahams et.al., 1980; Shapiro and Abrahams, 1981). The description presented here is in agreement with these conclusions, cf figure 16, however the logarithmic divergences in the free energy are exponentiated to give power law dependencies in time equivalent to an anomalous dimensionality in the spatial property (Hohenberg and Halperin, 1977). In this way the logarithmic frequency and length dependence of Abrahams et.al. (1980) will be modified into a power law behaviour (Mott and Kaveh, 1981).

6.4 Distribution of hopping times

Bernasconyi and his co-workers (see Bernasconyi et.al., 1979) have developed this approach in a series of papers in which the Mori formalism has been utilised together with a static distribution of inter-site hopping rates. It was shown that when this distribution diverged for small rates anomalous conductivity ensued of the form of equation (26), with a non-universal index p whose value depended on the form of the divergence in the hopping rate distribution. Alternatively a D.C. conductivity was found when the distribution was bounded.

This approach bears some superficial resemblance to that presented here in that a self-consistent solution to equation (4) results in the Mori formalism and the distribution used were of the type to produce an infra-red divergence. However their concept of a static spatial distribution of hopping rates is quite distinct from that of the present work. The difficulty with such a concept is that it has not been related to the material structure except insofar as a Poisson distribution of site separations leads to a similar result in spin systems (Theodoru and Cohen, 1979). Because of the lack of a relationship with structure the two regimes given by equations 26 (a) and (b) were not identified theoretically. As a consequence the low frequency dispersion regime in Hollandites was taken to be a D.C. conductivity (Bernasconyi et.al., 1979) and only the high frequency regime was analysed.

Because the hopping rate distribution was assumed to be due to a distribution of activation energies a temperature dependent value of n was obtained which was predicted to become zero at $T \approx 410$ K, at which temperature the system became D.C. conducting through a mobility transition. The experimental data for the Hollandites, figure 7, show no such temperature dependence with the same low frequency dispersion characteristics observable up to 863 K.

The experimental data given by these authors in support of their model was obtained in a small frequency window, $10^4 - 10^6$ Hz, and over a narrow range of temperatures, 150 K to 213 K. Since ω_c moves to higher frequencies with increasing temperature the low frequency dispersion regime of equation (26a) will move towards the lower part of the frequency window effectively reducing the observed value of n and giving the form of result observed. If this regime were taken to be a D.C. conductivity then a continuous crossover would occur as it moved into the frequency window. The conclusions drawn by these authors with respect to the temperature dependence of the conductivity are therefore erroneous and caused by the limited range of measurements made.

7. Conclusions

A new model of anomalous low frequency dispersion has been presented which relates the mechanism directly to the disordered material structure which is described in terms which link the local order and the long range order. The two power law regimes in frequency have been identified with fluctuations in the structural order on a cluster scale and on an inter-cluster macroscopic scale.

The behaviour can also be expected in low dimensional disordered materials which possess a potential electronic conductivity. In this case the cluster can be identified with an electronic wave-packet spread over a number of donor sites and possessing an internal structure due to the local order. The polarised cluster can therefore be thought of as an intermediate, rather than a Wannier, exciton. Since the anomalous transport will be cut-off at long times by electron diffusion ($t > 10^{-10}$ s) and at short times by quantum effects ($t < 10^{-13}$ s) the restricted time/frequency range available will render it likely to be observed in electronic systems of low dimensionality. The long time limit in such systems has been shown to be of the conventional diffusion limited form. The relation between electrical noise and the anomalous low frequency dispersion has been examined and in the diffusion limited case gives a power noise rigorously proportional to the inverse frequency. Variations from this characteristic can be taken as evidence for a non-perfect diffusion in the system under examination.

It has been clearly demonstrated for non-electronic charge carriers, such as protons, that the time scale over which the anomalous properties will be observed occurs over much longer times than for the electronic case and can conveniently be determined through the noise power/frequency relationship.

It has been shown that even with transmitting electrodes the systems investigated here exhibit a sample size dependent conductivity, decreasing with increasing size. The quantitative variation of the conductivity with size has not been investigated here as it will depend on the properties of the specific system examined. It has also been shown that measurement of the conductivity alone, or the loss alone, may not be sufficient to discriminate between low frequency dispersion and D.C. conductivity. It is

considered that this observation may have serious consequences in the evaluation of solid fast ion conductors as power cells. The relation between the anomalous dispersion and electrical noise has been examined and found to have a common origin and related power indices.

Low frequency dispersion is known to occur in bio-systems such as hydrated proteins (Bone et.al., 1981) and the in-vivo response of plants to electrical stimulus (Hart, 1981). It can be expected that the interpretation of this phenomenon which has been presented here will assist in a more comprehensive understanding of some of the features of these fields.

It requires to be emphasised that the model developed here need not be restricted to electrical transport. When the inter-cluster exchange processes carry no charge a relaxation loss peak will be observed dielectrically, but if their motions are conjugate to an applied field such as pressure then a flow will result. The separation of the site motions into intra-cluster and inter-cluster has been recognised by Cotterill and Tallon (1980) who have pointed out that the motion of an atom along a single coordinate in a liquid can be simultaneously a vibration and a transportation. We expect the basic concepts of the model to be of general applicability and of use in a number of branches of science dealing with imperfect transport in disordered systems. Because the model connects the microscopic structure to the macroscopic stochastic system with complete generality of form it is equally applicable to solids and liquids alike.

References

- Abrahams E., Anderson P. W. and Ramakrishnan T. V., 1980, *Phil.Mag.B.*, 42, p 827
- Almond D. P., West A. R. and Grant R. J., 1982, submitted for publication
- Auckland D. W. and Cooper R., 1974, *CEIDP*, p 71
- Austin I. G. and Mott N. F., 1969, *Adv. in Phys.*, 18, p 41
- Barham P. J. and Keller A., 1977, *Jnl.Matl.Sci.*, 12, p 2141
- Bernasconyi J., Beyeler H. U., Strassler S. and Alexander S., 1979 *Phys.Rev.Lett.*, 42, p 819
see also J.Bernasconyi, W.R.Schneider and W.Wyss, 1980, *Zeit.fur Physik.B.*, 37, p 175
- Alexander S and Bernasconyi J., 1979, *J.Phys.C.*, 12, p L1
- Bernasconyi J., Alexander S. and Orbach R., 1978, *Phys.Rev.Lett.*, 41, p 185
- Beyeler H. U., 1976, *Phys.Rev.Lett.*, 37, p 1557
- Binder K., Stauffer D and Muller-Krambar H., 1975, *Phys.Rev.*, B12, p 5261
- Bodiakin B., 1982, Ph.D. Thesis, University of London
- Bone S., Eden J. and Pethig R., 1981, *Intl.Jnl.Quant.Chem.*, Quant Biol.Symp., 8, p 307
- Bystrom A. and Bystrom A. M., 1950, *Acta.Cryst.*, 3, p 146
- Carslaw H. S. and Jaeger J. C., 1947, "Conduction of Heat in Solids", Oxford Univ.Press., Oxford
- Chester C. V., 1963, *Rep.Prog.Phys.*, 26, p 411
- Cotterill R. M. J. and Tallon J. L., 1980, *Chem.Soc.Far.Disc.*, 69, p 241
- Cole K. S. and Cole R. H., 1941, *Jnl.Chem.Phys.*, 9, p 341
- Dissado L. A., 1982, *Physica Scripta*, in press
- Dissado L. A. and Hill R. M., 1979, *Nature, Lond.*, 279, p 685
1980, *Phil.Mag.B.*, 41, p 625
1981, *Jnl.Matl.Sci.*, 16, p 638
1982, U.S.Army Research Dev. & Stand.Group
Interim Report I.
- Doyle B., 1981, Ph.D. Thesis, University of London
- Eden J., Gascoyne P. R. C. and Pethig R., 1980, *Jnl.Chem.Soc.Far.Trans.2.*, 76, p 426
- Elliott S. R., 1977, *Phil.Mag.*, 36, p 1291
- Feynman R. P. and Hibbs A. R., 1965, "Quantum Mechanics and Path Integrals", McGraw-Hill, New York
- Freund F., 1981, *Trends in Biochemical Sciences*, p 142
- Frost M. and Jonscher A. K., 1975, *Thin Solid Films*, 29, p 7
- Garton C. g., 1939, *Proc.Inst.Elec.Eng.*, 88, III, p 23
- Gupta M. S., 1977, "Electrical Noise: Fundamentals and Sources", IEEE Reprint Series, Wiley, New York
- Halperin B. I., Hohenberg P. C. and Ma S. K., 1972, *Phys.Rev.Lett.*, 29, p 1548
- Hart F. X., 1981, private communication
- Hohenberg P. C. and Halperin B. I., 1977, *Rev.Mod.Phys.*, 49, p 435
- Hill R. M., 1977, *phys.stat.sol.(a)*, 39, p 615
1978, *Nature, Lond.*, 275, p 96
1981(a), *Jnl.Matl.Sci.*, 16, p 118
1981(b), *phys.stat.sol.(b)*, 103, p 319
- Hill R. M. and Dissado L. A., 1982, *J.Phys.C.*, in press
- Hill R. M., Dissado L. A. and Jackson R., 1981, *J.Phys.C.*, 14, p 3915
- Hill R. M. and Jonscher A. K., 1982, *Contemp.Phys.*, submitted for publication
- Hopfield J. J., 1970, *Commun.Solid.State.Phys.*, 11, p 1522

- Joffrin J. and Levelut A., 1975, J.Phys.(Paris), 36, p 811
- Jonscher A. K., 1975, phys.stat.sol.(a), 32, p 665
 1977, Nature, Lond., 267, p 673
 1978, Phil.Mag., 38, p 587
- Jonscher A. K. and Frost M., 1976, Thin Solid Films, 37, p 267
- Jonscher A. K., Dissado L. A. and Hill R. M., 1980, phys.stat.sol.(b), 102, p 351
- Jonscher A. K., Deori K. L., Reau J-M. and Moali J., 1979, Jnl.Matl.Sci., 14, p 1308
- Jonscher A. K., Meca F. and Millany H. M., 1979, J.Phys.C., 12, p L293
- Kadanoff L. P., 1966, Physics, 2, p 263
- Kubo R., 1957, J.Phys.Soc.Jap., 12, p 570
 1962, J.Phys.Soc.Jap., 17, p 1100
- Maxwell J. C., 1954, "A Treatise on Electricity and Magnetism", Vol I., p 452, Dover Press, New York
- Mott N. F. and Kaveh M., 1981, J.Phys.C., 14, p L659
- McCrum N. G., Read B. E. and Williams G., 1967, "Anelastic and Dielectric Effects in Polymeric Solids", Wiley, London
- Ngai K. L., Jonscher A. K. and White C. T., 1979, Nature, Lond., 277, p 185
- Patashinskii A. Z. and Pokrovskii V. I., 1979, "Fluctuation Theory of Phase Transitions", Pergamon Press, Oxford
- Pender L. F. and Wintle H. J., 1979, Jnl.Appl.Phys., 50, p 361
- Pollak M. and Geballe T. H., 1961, Phys.Rev., 122, p 1742
- Ramdeen T., 1981, M.Sc. Thesis, University of London
- Reau J. M., Moali J. and Hagenmuller P., 1977, J.Phys.Chem.Sol., 38, p 1345
- Resibois P. and De-Leener M., 1966, Phys.Rev., 152, p 305
- Shablakh M., Hill R. M. and Dissado L. A., 1982(a), J.Chem.Soc.Far.Trans.2., 78, pp 625 and 639
- Shablakh M., Dissado L. A. and Hill R. M., 1982(b), J.Chem.Soc.Far.Trans.2., submitted for publication
- Shahidi M., Hasted J. B. and Jonscher A. K., 1975, Nature, Lond., 258, p 595
- Shapiro B. and Abrahams E., 1981, Phys.Rev., B24, p 4889
- Slater L. J., 1960, "Confluent Hypergeometric Functions", CUP, Cambridge
 1966, "Generalised Hypergeometric Functions", CUP, Cambridge
- Theodoru G. and Cohen M. H., 1979, Phys.Rev., B19, p 1561
- Thouless D. J., 1973, J.Phys.C., 6, p L49
- Wagner K. W., 1914, Arch.Elektrotech., 2, p 371
- Wilson K. G. and Kogut J., 1974, Phys.Repts., 12C, p 75
- Witkowski A. and Wojcik M., 1973, Chemical Phys., 1, p 9
- Wong J. and Angell C. A., 1976, "Glass Structures by Spectroscopy", Dekker, New York

Legends

Figure 1. Representation of anomalous low frequency dispersion with $p = 0.95$ and $n = 0.7$. The frequency ω_c indicates the relaxation rate and the parallelism of the real and imaginary components in this log/log presentation can be clearly seen for both $\omega > \omega_c$ and $\omega < \omega_c$. The dotted curves show the D.C. case and the chain dotted line defines a frequency above which the response may be confused with D.C. behaviour.

Figure 2. (a) Projection of the Hollandite structure onto the (001) plane. The barred ions are situated at $z = 0.5$ and the O and K symbols represent the oxygen and potassium sites, respectively, with the M sites containing either Ti or Mg. (After Bystrom and Bystrom, 1950)

(b) The developed Hollandite structure showing two unit cells in the z direction. One of the channels within which the potassium ions can move in the presence of ion vacancies is indicated.

(c) Representation of the channel sequences combined in groups to give the channel correlation length of 35 Å (Beyeler, 1976). The empty cells indicate vacancies.

Figure 3. (a) Schematic representation of three inter-cluster exchange mechanisms which transport a charge over the same range. The arrows show the ion transport and the signs give the charge densities produced.

(b) A schematic representation of a spatially uniform polarisation (ii) in a typical cluster (i) which indicates the equivalence to a whole cluster dipole with an effective charge δ . The ions and lattice counter-charges are shown for a system with 75% occupancy. The dashed lines indicate the site centres.

(c) Schematic representation of all the system processes. (i) Spatially uniform cluster polarisation ; (ii) Some inter-cluster exchange processes and (iii) Cluster relaxation processes.

(d) Schematic representation of fully coupled, out of phase, ion displacements showing the equivalence to the vibration of the effective cluster dipole.

Figure 4. The function $\psi(t)$ describing the time development of the prepared state for a range of values of p . As p approaches unity the oscillations increase in amplitude and for $p \geq 0.9$ the first oscillation, at least, goes negative.

Figure 5. A schematic diagram showing the decay and growth of the fluctuations. Initially it has been assumed that the individual elements are all at their average value in the prepared state and the fluctuations give rise to the steady-state distribution shown on the right-hand side. The diagram has been constructed for $p = 0.3$ and indicates both the gaussian approach to zero time and the resonance-like behaviour for ζt being of the order of unity as shown in figure 4.

Figure 6. The probability density functions for a range of values of the index p . The fluctuation scale has been normalised to the average value for each distribution.

Figure 7. Master curves of susceptibility as a function of frequency for (a) Hollandite of composition $K_2Al_2Ti_6O_{16}$ (b) Hollandite of composition $K_{1.8}Mg_{0.9}Ti_{7.1}O_{16}$ and (c) humid sand. The continuous functions have been obtained from equation (25) with the values of p and n determined as (a) $p = 0.92$, $n = 0.7$ (b) $p = 0.92$, $n = 0.6$ and (c) $p = 0.8$, $n = 0.94$. The curves have been displaced for clarity. The data for (a) and (b) was taken from Jonscher et.al., (1981) and for (c) from Shahidi et.al. (1975)

Figure 8. Master curve of the susceptibility of a glass (Allied base glass) from the data of Doyle (1981). The continuous curves have been determined from equation (25) with $p = 0.993$ and $n = 0.5$. The diagram is scaled at 800 K.

Figure 9. Master curve for the loss component of susceptibility for hydrated bovine serum albumin from the data of Eden et.al. (1980). The normalisation has been carried out in terms of the percentage water adsorbed and the diagram is scaled at 8.7 wt%. The normalisation of both the anomalous dispersion and the loss peak clearly indicates a common basis for both processes.

Figure 10. The real and imaginary components of the permittivity of the plastic crystal state of cyclopentanol showing a loss peak at high, relative, frequencies and pure D.C. conductivity with no dispersion in the capacitance at low frequencies. The diagram is scaled at 180 K and the data is taken from Shablakh et.al. (1982b)

Figure 11. The loss component of the susceptibility for the crystal state II of cyclopentanol showing a weak loss peak at high, relative, frequencies which does not normalise with the anomalous dispersion. The plot is scaled at 110 K and the data is taken from Shablakh et.al. (1982b).

Figure 12. The loss component of the susceptibility in the crystal III structure of cyclohexanol. Over the normalisation temperature range of 190 K to 218 K the weak loss process embedded in the low frequency dispersion remains in its relative position showing that the two processes have a common basis. The data is taken from Shablakh et.al. (1982b). Scaled at 218 K.

Figure 13. The permittivity of a doped glass (J 22) in the temperature range between 490 K and 1066 K. The normalised plot shows the lower frequency range of an anomalous low frequency dispersion with evidence of saturation in both the real and imaginary components at the lowest reduced frequencies. The continuous curves were obtained from equation (25) with $p = 0.92$ and $n = 0.4$. The plot is scaled at 1066 K. (Doyle, 1981)

Figure 14. The permittivity of egg lecithin measured at two temperatures. At the higher temperature the onset of the diffusion controlled process, with $p = 0.5$, can be seen together with the distortion this introduces into the real component in the anomalous low frequency dispersion region. The continuous curves have been determined from equation (25) with $p = 0.86$. The two sets of data have been displaced for clarity (after Jonscher, 1978).

Figure 15. The anomalous low frequency dispersion relationship of equation (25) plotted in the form of A.C. conductivity from equation (36), for a range of values of p . As p approaches unity the conductivity becomes indistinguishable from the frequency independent D.C. form.

Figure 16. Schematic representation of the average response current as a function of time in the region of $t = \omega_c^{-1}$. An exponential relaxation is shown for comparison as is the region of response that leads to the observation of loss peaks. The perfect inter-cluster transport case, with $p = 1$, is the D.C. like behaviour shown in figure 15.

Figure 17. Typical anomalous low frequency dispersion presented in the form of the dielectric modulus where $M(\omega) = \{\epsilon(\omega)\}^{-1}$. The diagram illustrates the approach of both the real and imaginary components to zero at zero frequency and the presence of a peak in the imaginary component of the modulus. This diagram should be compared with figure 1, which presents the same information in susceptibility representation. The high frequency permittivity ϵ_∞ , which dominates the high frequency real component of the modulus, has been taken as unity in the normalised scale used. $p = 0.95$ and $n = 0.7$

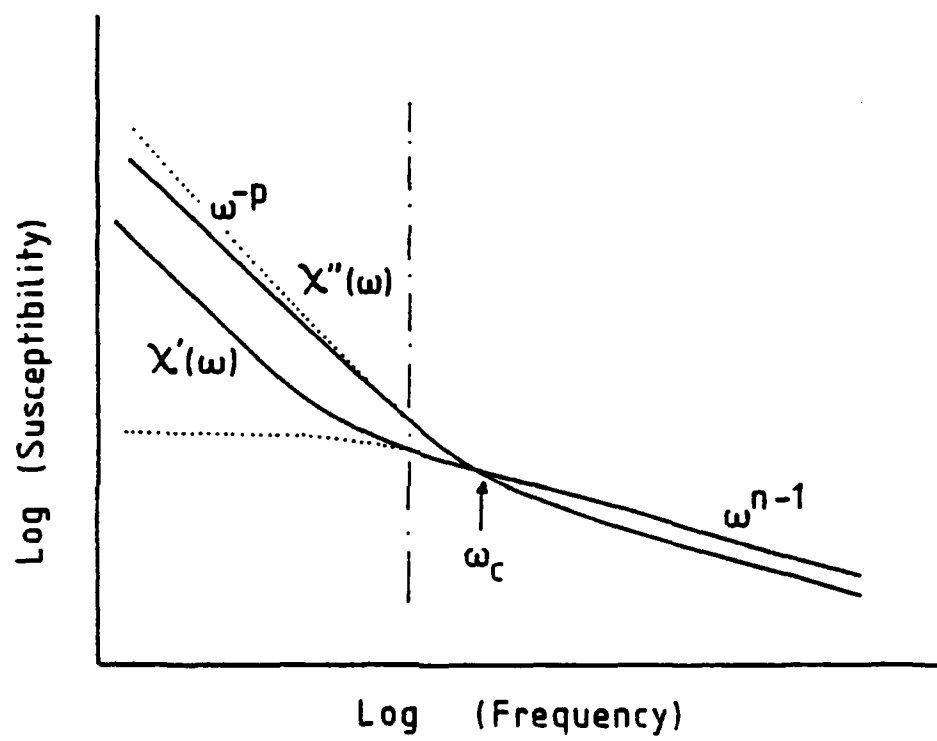
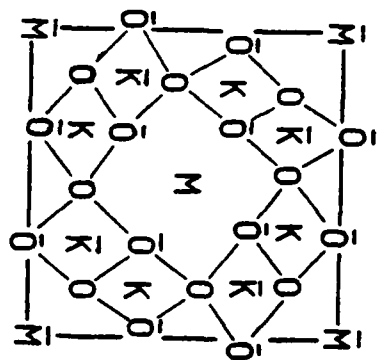
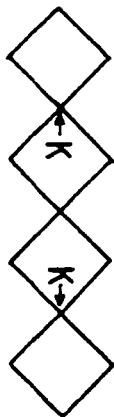


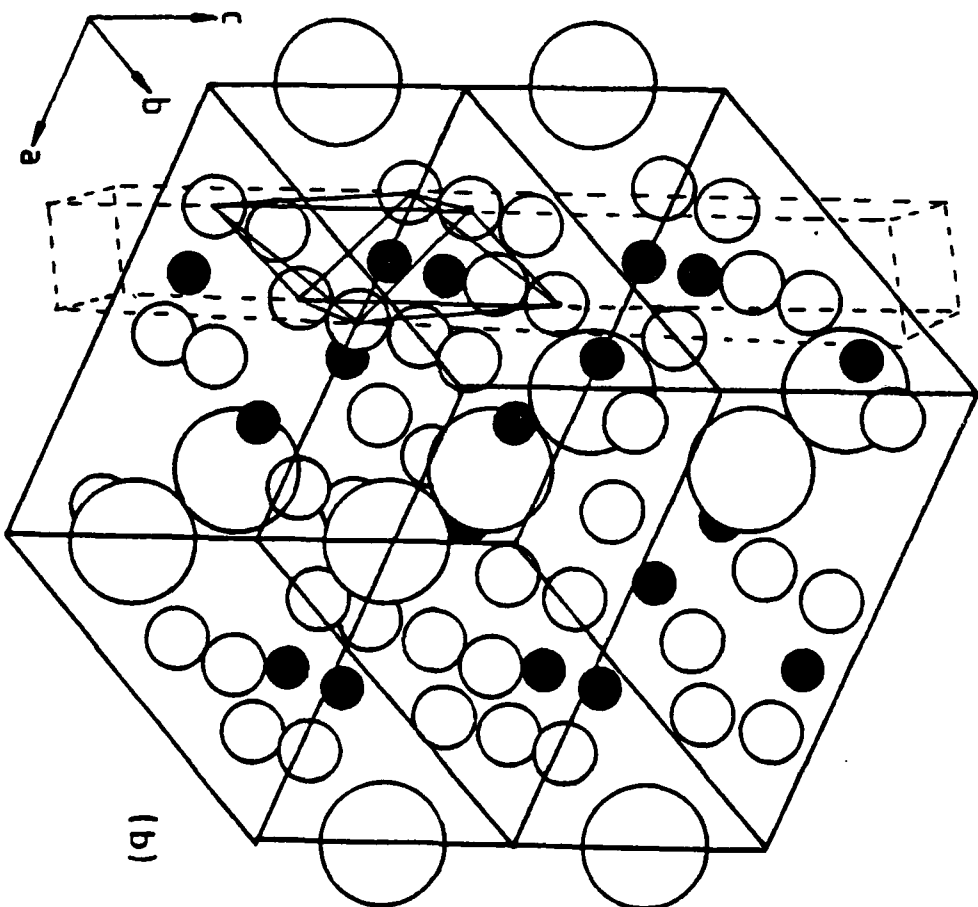
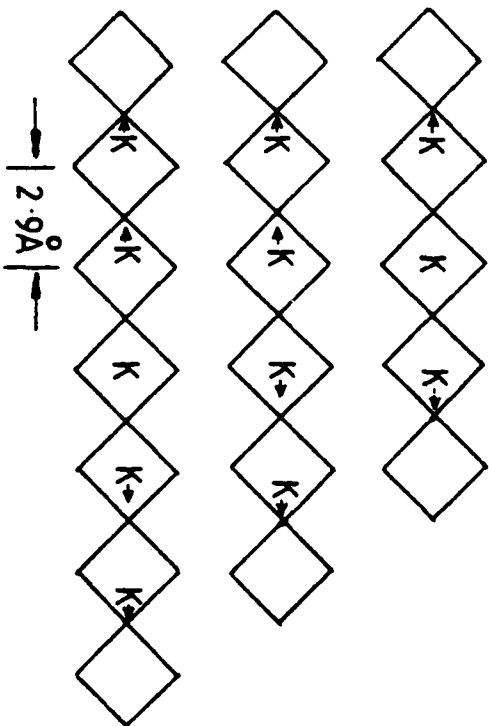
Figure 1.



(a)

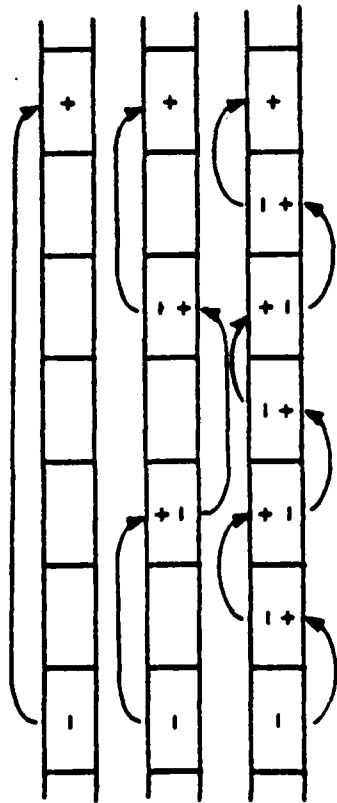


(c)

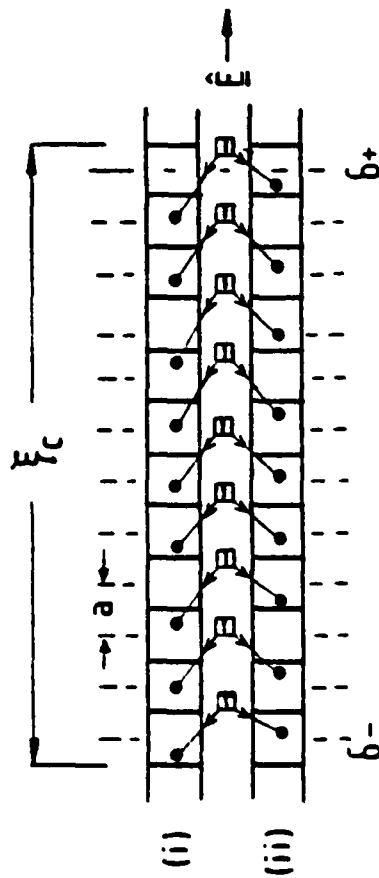


(b)

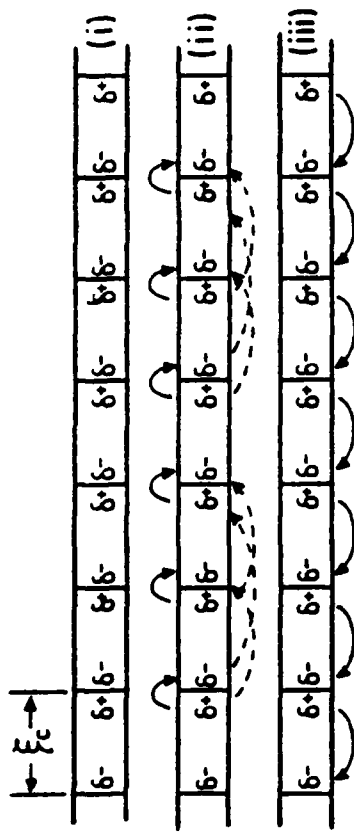
Figure 2.



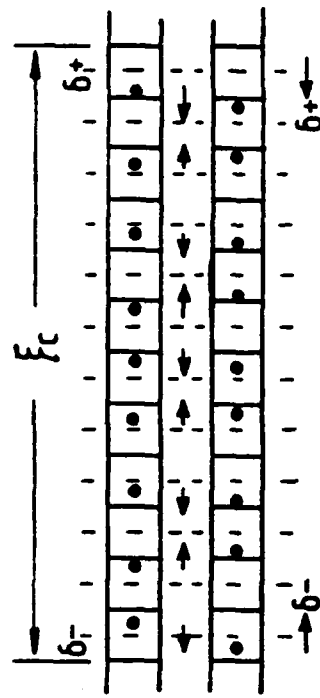
(a)



(b)



(c)



(d)

Figure 3.

Figure 4

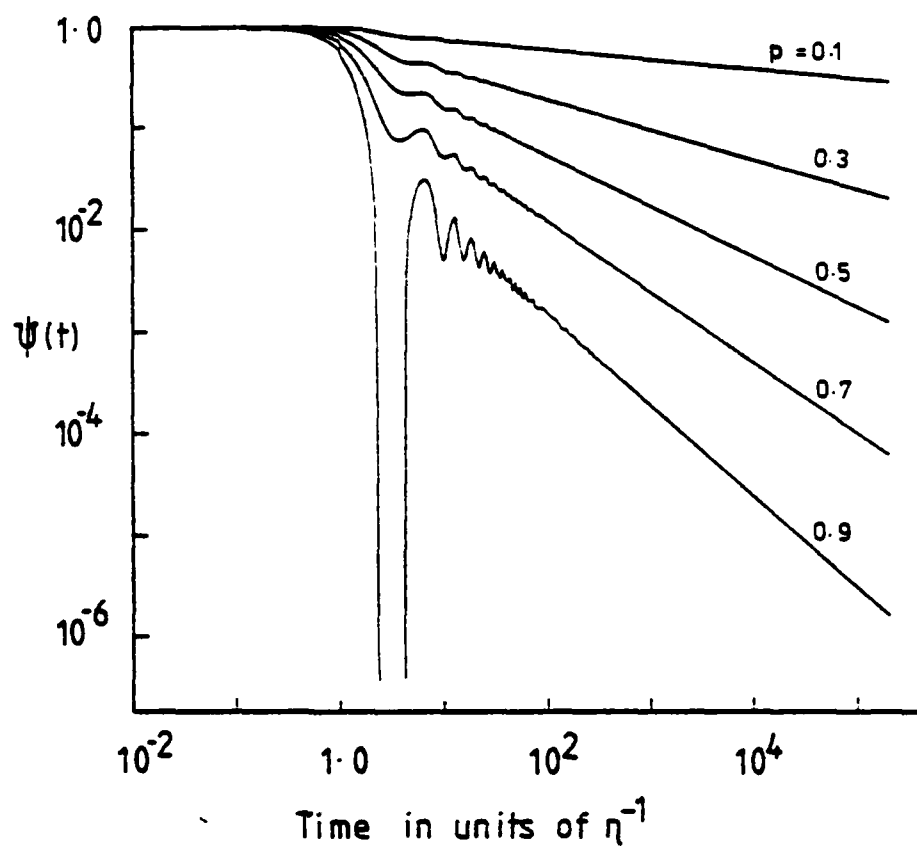


Figure 5

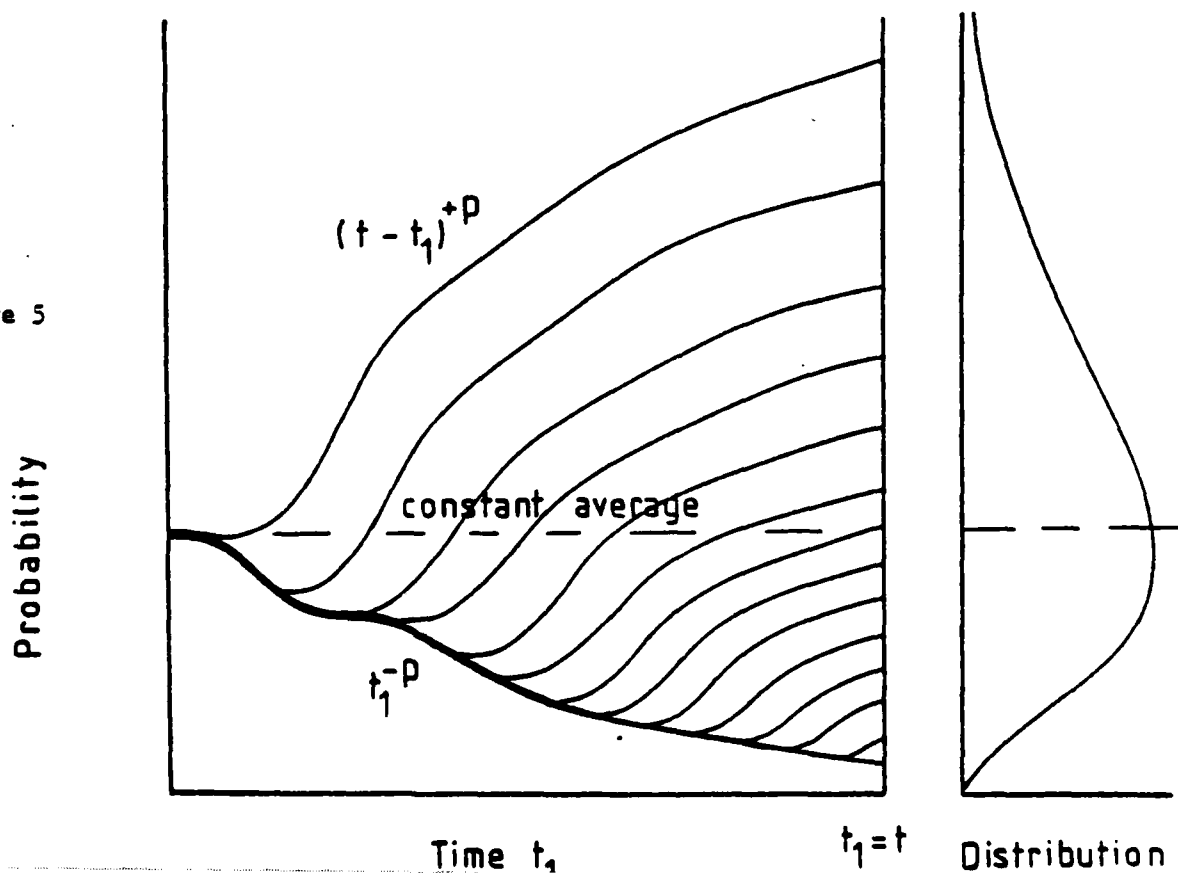
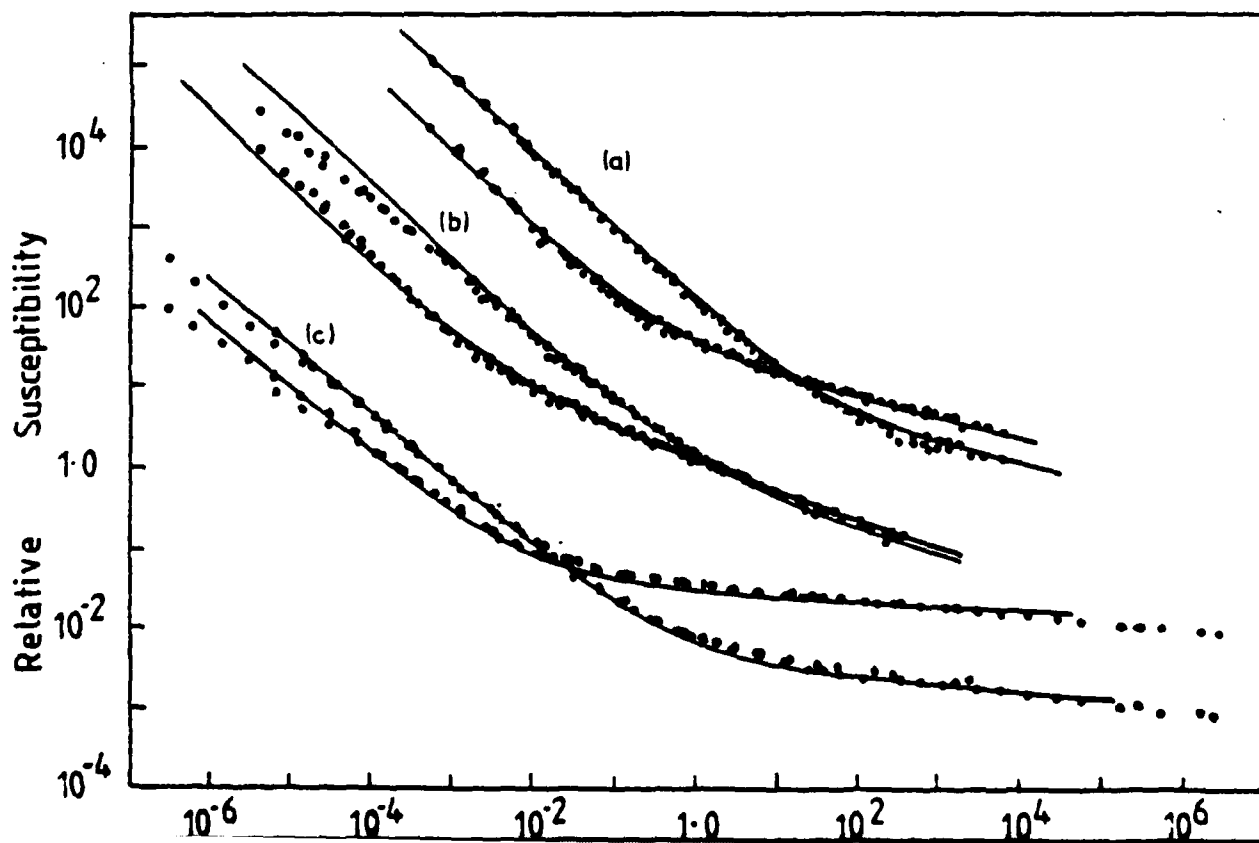
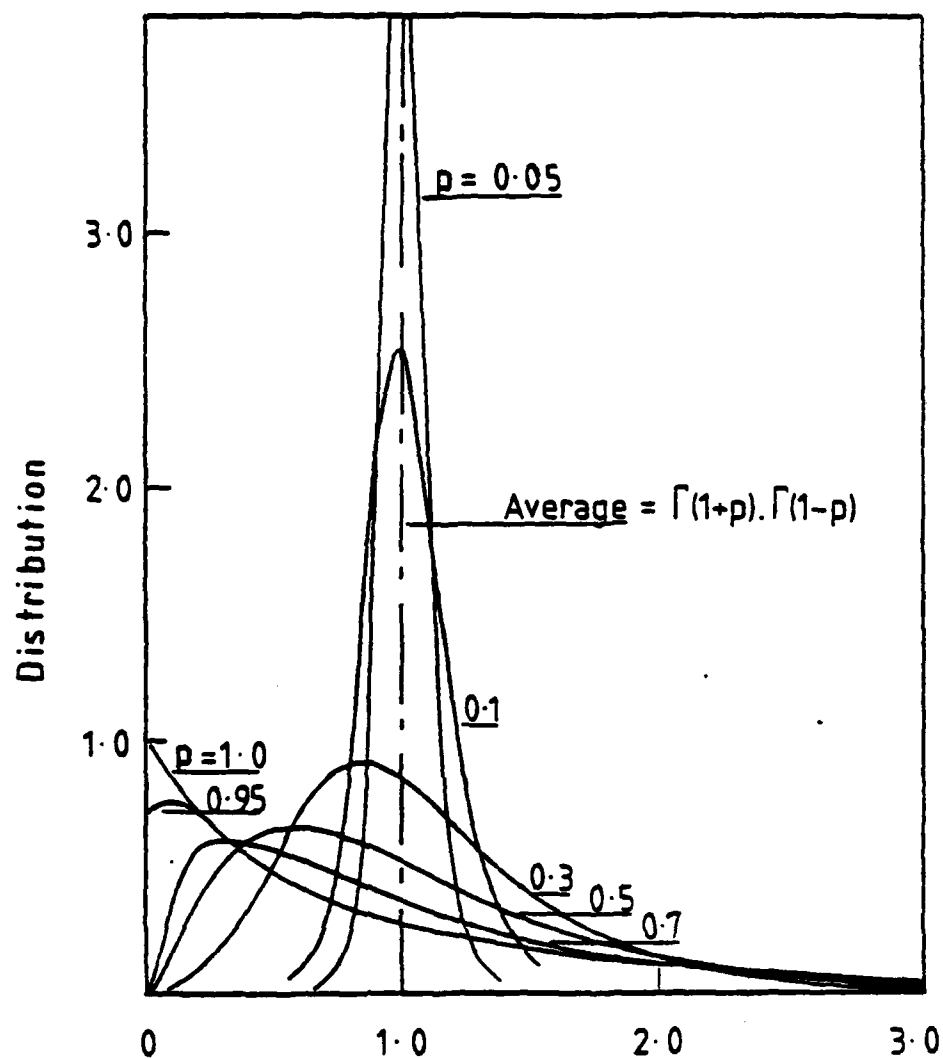


Figure 6



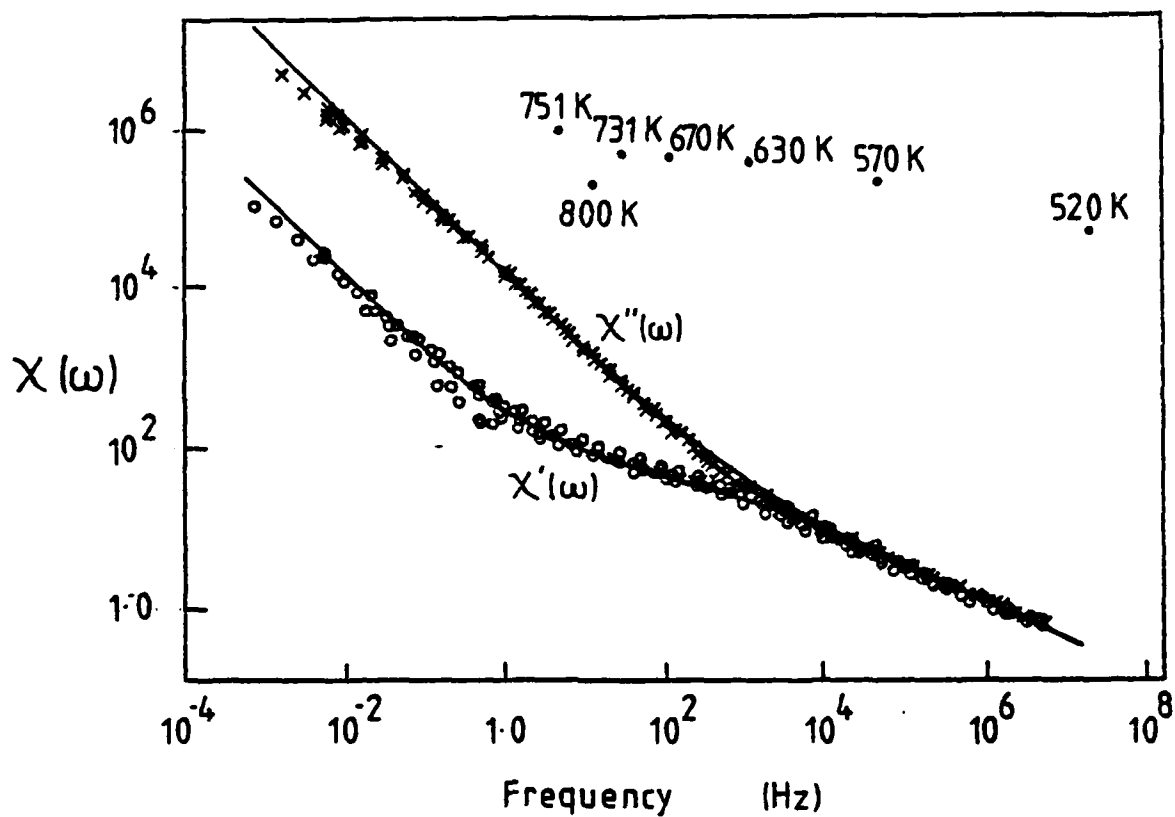


Figure 8.

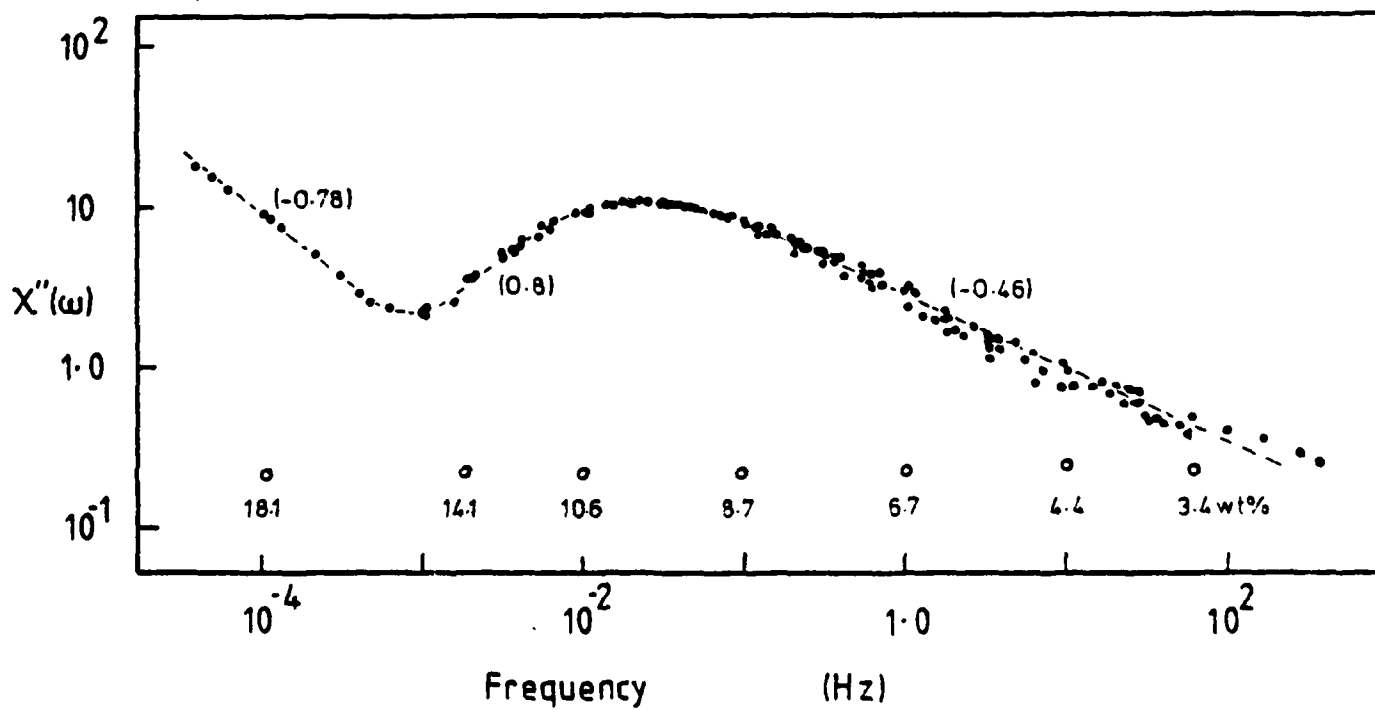


Figure 9.

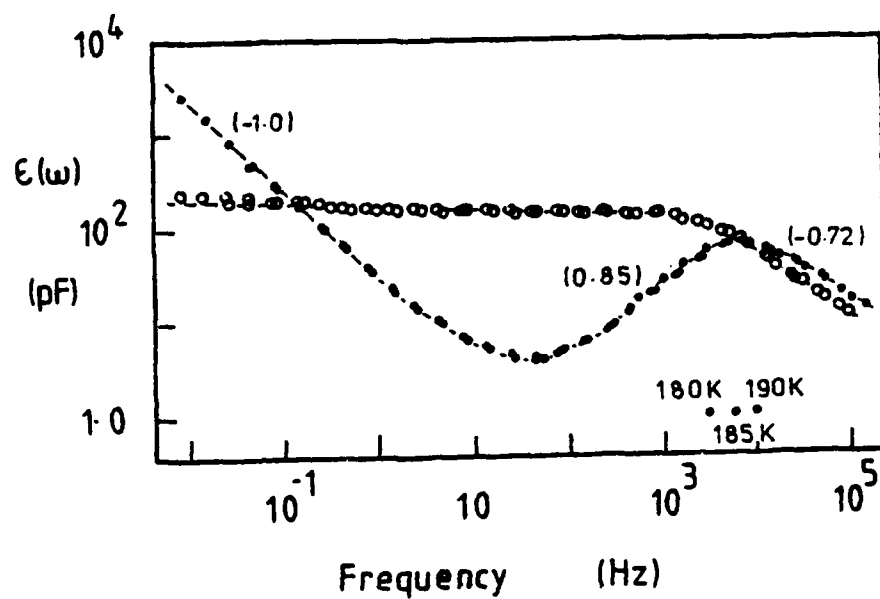


Figure 10

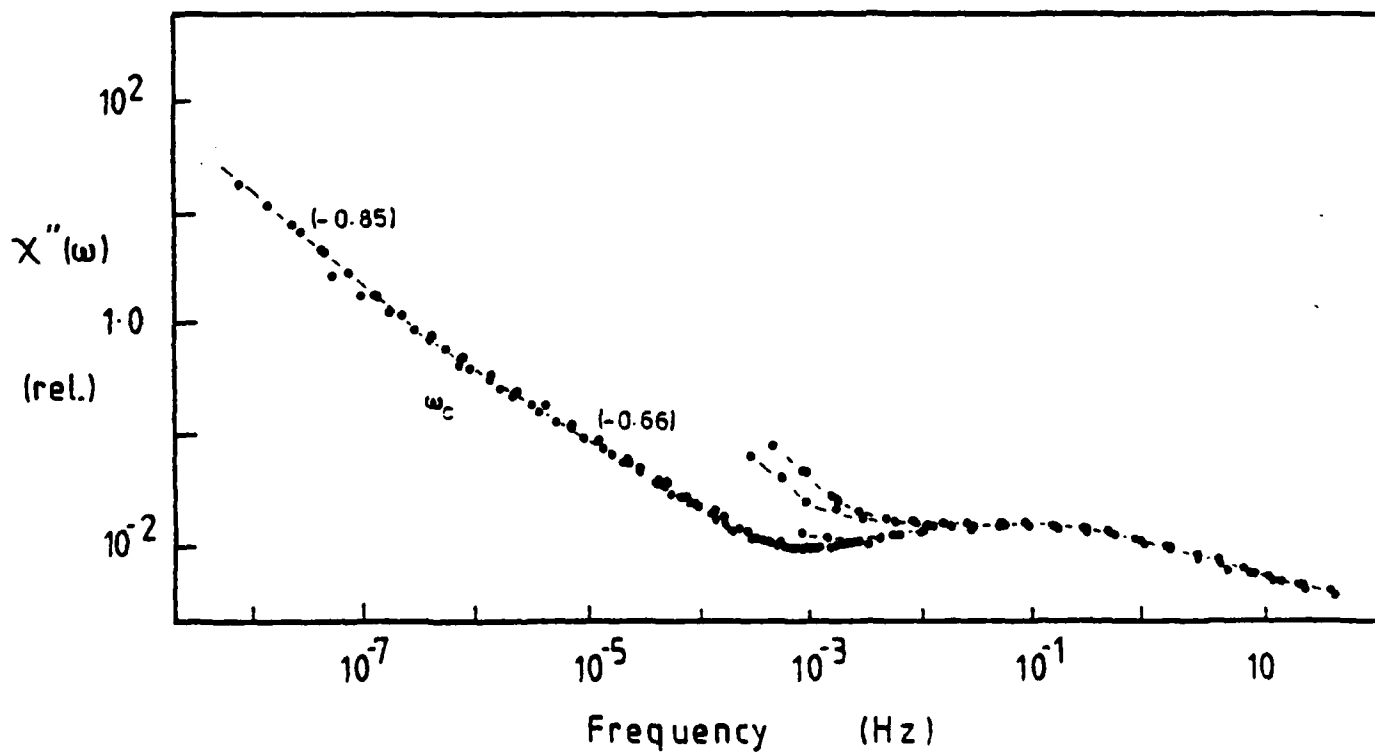


Figure 11.

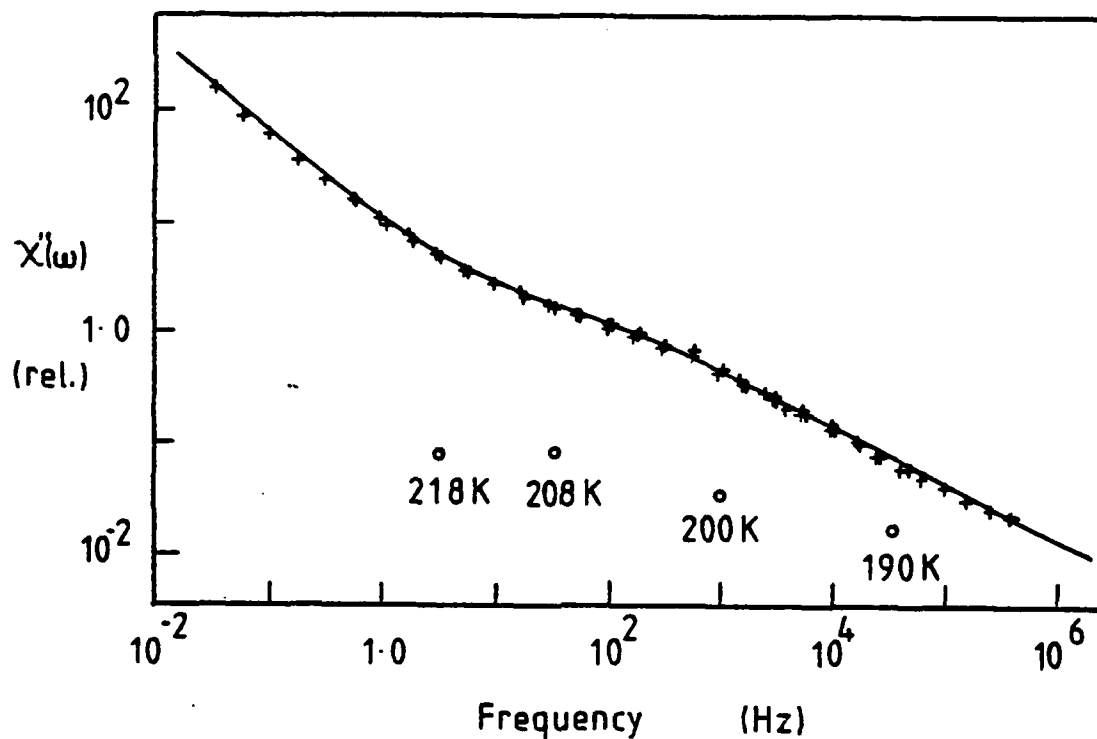


Figure 12.

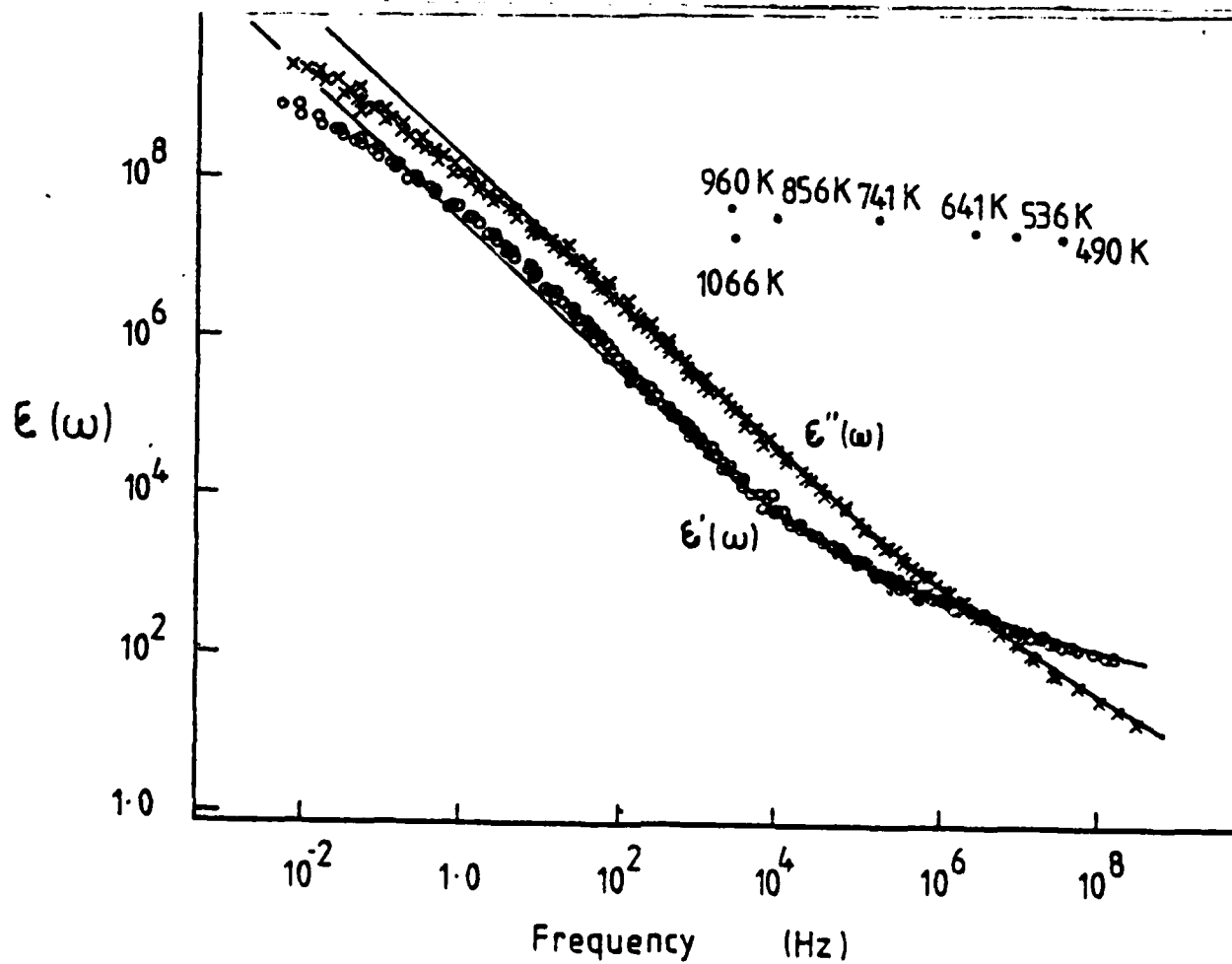


Figure 13.

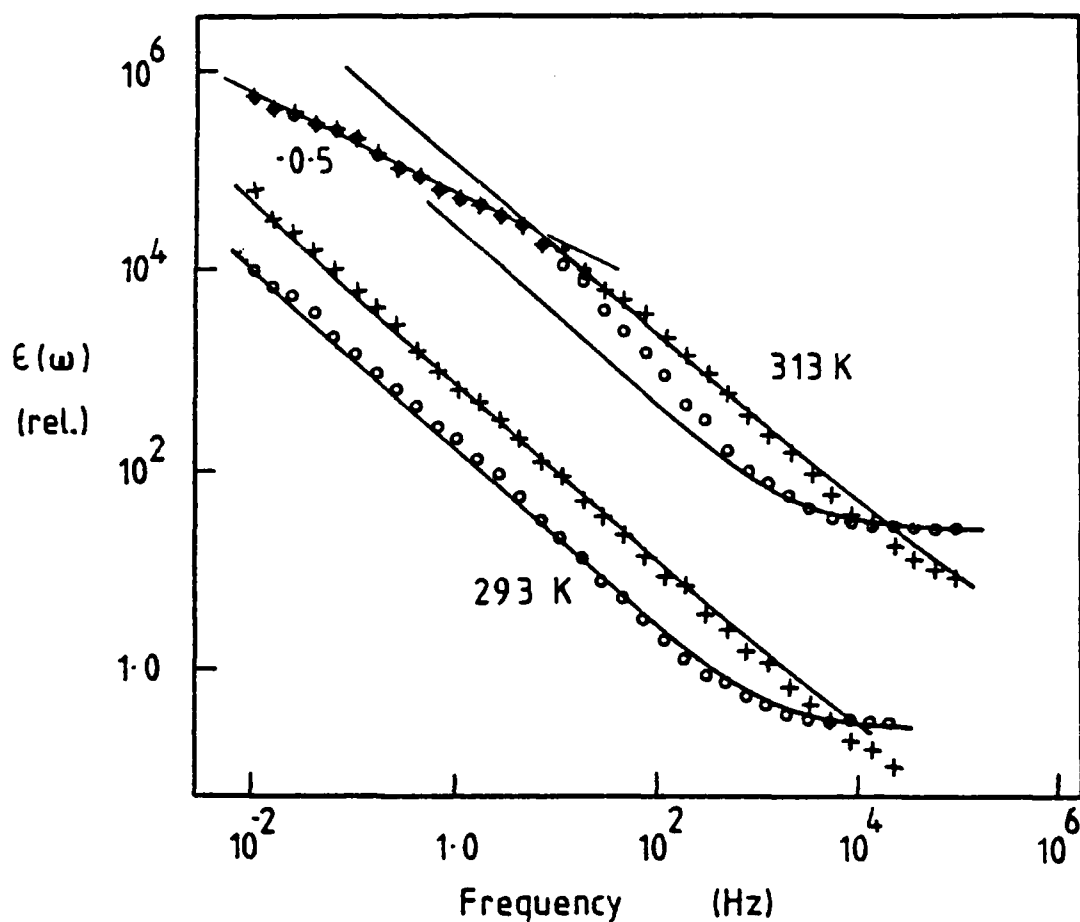


Figure 14.

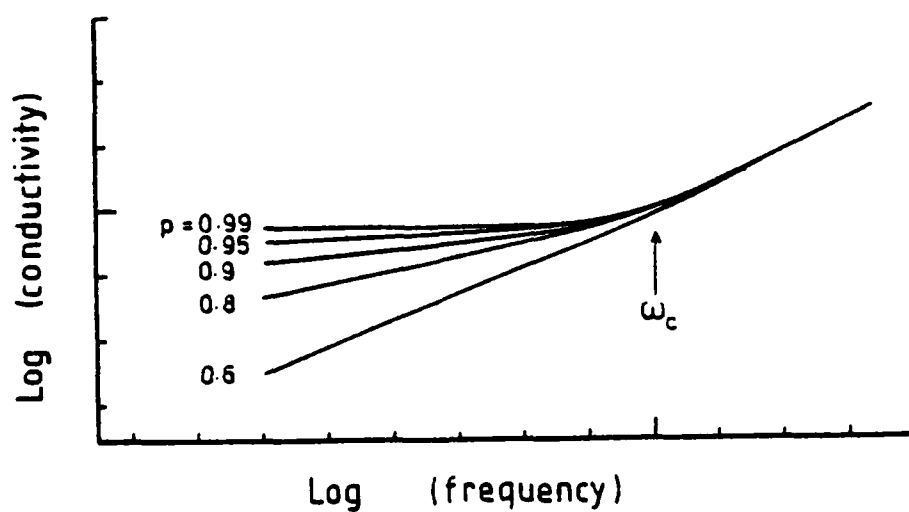


Figure 15.

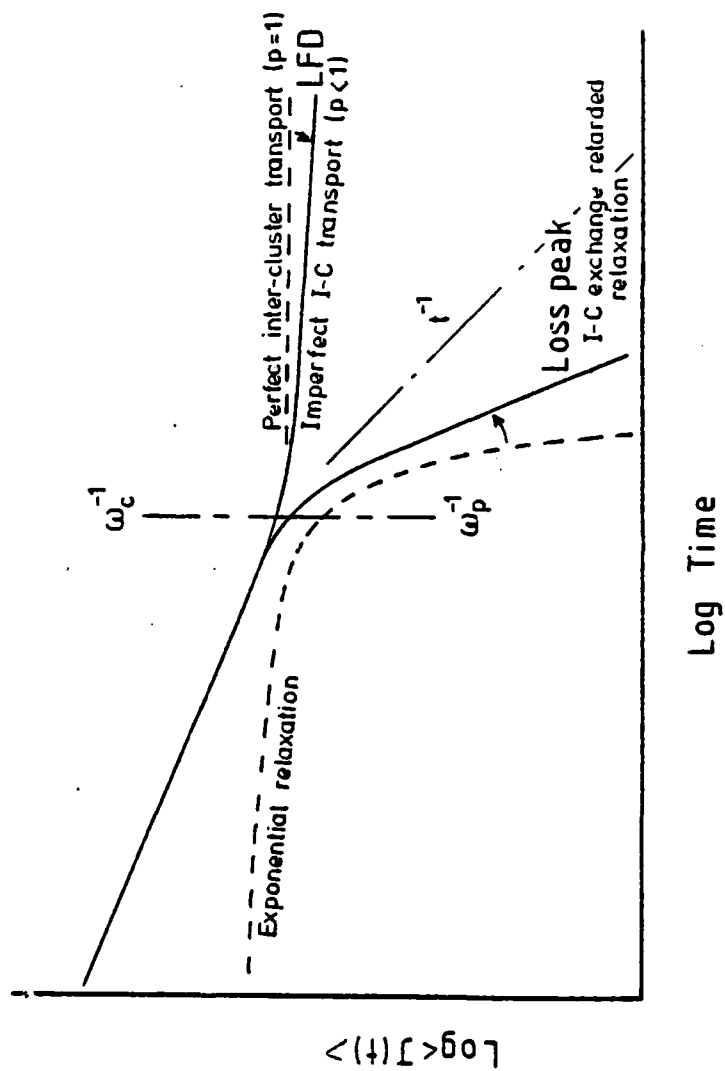


Figure 16.

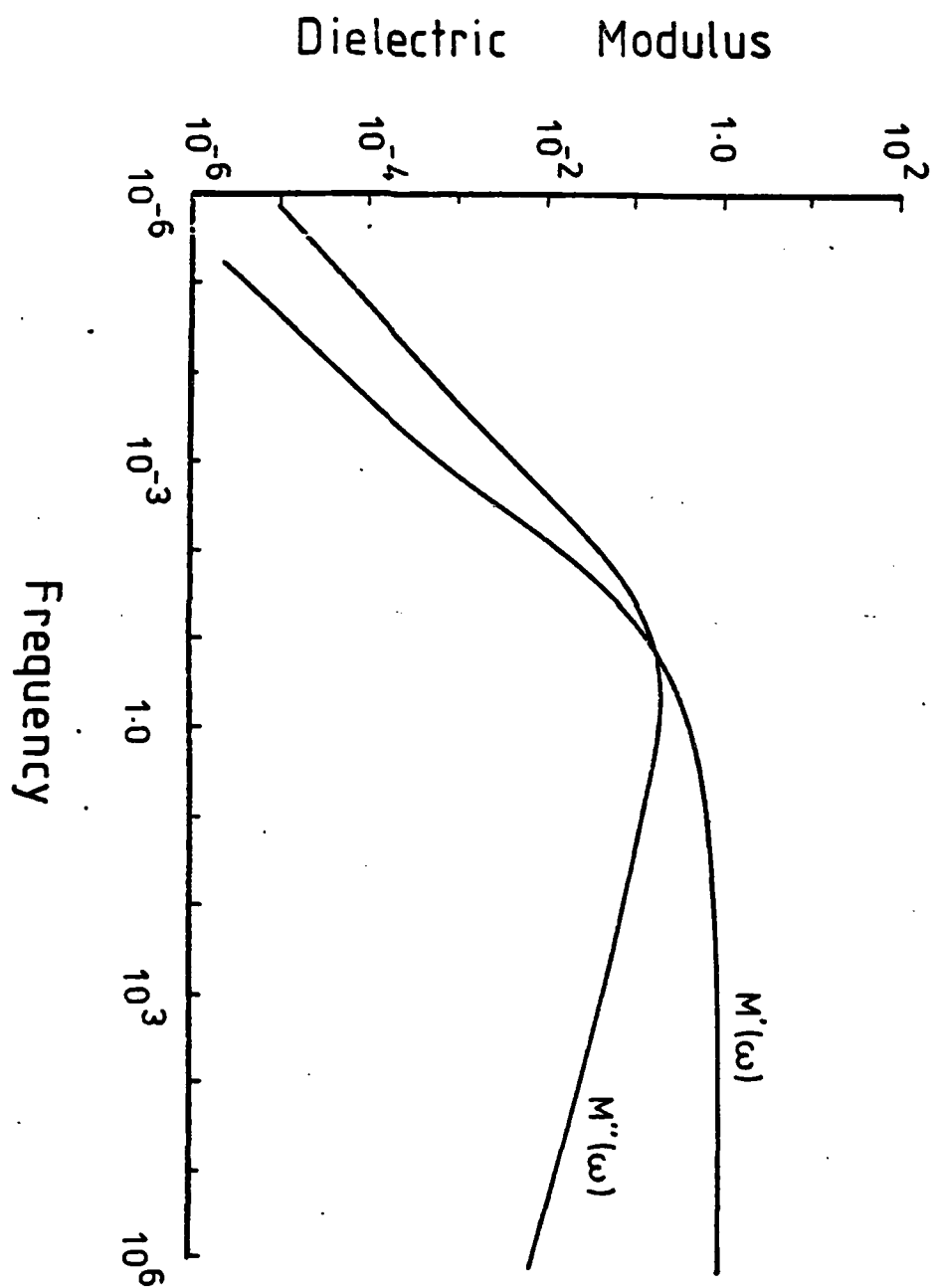


Figure 17

Theory of Many-Body Effects in Sub-Microelectronic
Systems I

Ferroelectric Response of Dopants in Finite Grain
Sized Perovskite Ceramics.

L. A. Dissado and R. M. Hill

Chelsea College, Department of Physics, University
of London, Pulton Place, London SW6 5PR

Abstract

The experimental data from a dielectric investigation of a series of doped ceramic ferroelectrics has been examined in order to determine whether the data showed effects due to the finite size of the ordered grains. It has been found that the order of the ferroelectric-paraelectric transition is affected by the grain size and it is pointed out that this has consequences on the mode structure of the materials. No direct evidence was found for correlation length limitations but the correlation lengths in the samples examined was determined as of the order of thirty lattice spacings.

Introduction

The aim of this study was to examine experimental data in order to determine whether the effect of finite sample size could be discerned. To this end we have chosen to look at the available data¹ on a doped ceramic ferroelectric which had been examined in this laboratory¹ through its dielectric susceptibility, $\chi(\omega)$, in the frequency range between 10^{-3} Hz and 10^4 Hz over a wide range of temperatures about the critical Curie temperature, T_c . The reason for this choice was two-fold. Firstly a body of theory² exists which predicts that those properties that formally diverge at the critical temperature, such as the dielectric susceptibility and the relaxation time, $(\omega)^{-1}$, saturate when the correlation length, ξ , becomes equal to the finite size, L , of the sample. Secondly the ceramic was composed of finite sized grains with an average diameter that was dependent on the method of preparation and of the concentration of the uranium dopant that had been introduced. The range of grain diameters available was from $2.5\mu\text{m}$ to $24\mu\text{m}$. Thus the system afforded the possibility of examining the predictions of the correlation length theory. The characteristics of the samples used are listed in Table I.

The theoretical predictions can be summarised by stating that when $\xi \geq L$ the correlation length in the diverging expressions can be replaced by L . Thus:

$$\chi(\omega=0) = (\xi)^{2-\eta} \quad \text{with } \xi = (|1 - T/T_c|)^{-\tau} \quad (1)$$

$$\text{becomes} \quad \chi(\omega=0) = (L)^{2-\eta} \quad (2)$$

$$\text{and} \quad \omega_p = v_o(\xi)^{-z} \quad (3)$$

$$\text{becomes} \quad \omega_p = v_o(L)^{-z} \quad (4)$$

$$\text{with} \quad \chi(\omega) = \chi(\omega=0) F(\omega/\omega_p) \quad (5)$$

where $F(\)$ is a complex function of the scaled frequency ω/ω_p . Expressions (1) to (5) give a series of relationships that can be examined experimentally.

Analysis of Experimental Data

The experimental data showed the presence of two loss peaks in the frequency window used for observation¹. Superimposed on the loss peaks was a substantial D.C. conductivity which, in the frequency domain, gives a loss decreasing with increasing frequency. The small value of the susceptibility increment associated with the loss process, $\Delta\chi'(\omega)$, and the sensitivity of the magnitude of the increment to dopant concentration identifies the observed response as arising from regions of the samples which are affected by the impurities. The true ferroelectric response occurred at frequencies higher than those measured but a good estimate of the ferroelectric susceptibility increment was obtained from the magnitude of the dielectric permittivity at 10^4 Hz. These values are plotted in figure 1,

as a function of temperature, for all five samples that had been investigated. In all but a single case the transition was found to be of first order, as can be seen by the discontinuities in the curves. The exception, sample RM35A, was the sample which had been prepared with only a single calcining to give particularly small particle sizes. The discontinuity in the traces for the other samples occurred at the critical temperature. Making recourse to the phenomenological expression for the free energy

$$G = G_{10} + \frac{a}{2} p^2 + \frac{b}{4} p^4 + \frac{c}{6} p^6 \quad (6)$$

in which b and c are essentially constant and a is given by

$$a = 4\pi(T - T_0)/C \quad (7)$$

When b is negative the transition is first order and the critical temperature is given by

$$T_c = T_0 + \frac{3cb^2}{64\pi c} \quad (8)$$

and there is the discontinuity in the susceptibility such that

$$\chi(T_c+) = 16c/(3b^2) \quad (9)$$

$$\text{and} \quad \chi(T_c-) = 4c/(3b^2) \quad (10)$$

$$\text{hence} \quad \{\chi(T_c+)\}/\{\chi(T_c-)\} = 4 \quad (11)$$

Approximately this value has been observed in all the samples except those containing 0.4% uranium, RM35A for which there was no discontinuity and RM35B for which the discontinuity was smaller, approximately two.

The case in which no discontinuous transition can be seen can be characterised by a positive value of b in equation (6), and hence is of second order. In this case there is an infinity in $\chi(\omega=0)$ at T_c , which is equal to T_0 , of the form

$$\{\chi(\omega=0)\}^{-1} = \frac{4\pi}{C} (T - T_0) \quad T > T_0 \quad (12a)$$

$$\{\chi(\omega=0)\}^{-1} = \frac{8\pi}{C} (T_0 - T) \quad T_0 > T \quad (12b)$$

and the ratio of the gradients, $d(\chi)^{-1}/dT$, above and below T_c has a value of two as observed for sample RM35A.

Perovskites, such as those investigated here, are expected to show a displacive phase transition with a soft mode. The modification to a first order transition may be attributed to electro-striction^{2,5} which arises from the grain boundaries of the unclamped crystals and leads to the negative value for b . It therefore appears that the small grain size in sample RM35A

alleviates this effect and allows the second order transition to take place. It is generally considered that increases of dopant concentration decreases T_c through a reduction of T_0 caused by lattice strain. However the dip in T_c for the larger particle sized, double calcined, 0.4% uranium sample (RM35B) might be due to a reduction in the magnitude of b , which then becomes positive for the small grain sized, single calcined, sample of the same concentration of dopant.

As stated earlier at lower frequencies than the ferroelectric process two loss peaks could be delineated within a background of some D.C. conductivity. An anomalous low frequency dispersion which is due to restricted mobility of charge centres in the samples was also observed. The two loss peaks were even observed in the undoped sample. It is known, however, from the method of sample fabrication that the undoped material contains vacancy centres in the perovskite structure. Of the two loss processes it was only possible to study the lower frequency one in detail. It was found that this process was very sensitive to the dopant concentration, as indicated in figure 2. It seems likely, therefore, that this peak can be attributed to uranium atoms in the doped materials and that these lie at the same type of lattice sites as the vacancies in the un-doped sample. As the low frequency loss peak exhibited critical behaviour it would appear that these sites must lie within the ordered grains and are coupled to the ordering field of the host lattice. Insufficient data exists to allow any assignment to be made to the slightly higher frequency loss process.

Scaling Effects

The mean field theory outlined in equations (6) to (11) often gives an approach to a critical point such as T_c with incorrect values for the power exponents ν , n and γ ($= \nu(2-n)$). Different values for these exponents are predicted by more exact theories and are generally called scaling effects.

i Static Scaling

These are effects observed in the static susceptibility, which we have taken to be the permittivity at 10 Hz as regards the very high frequency ferroelectric process. The susceptibility exponents for this process are given in Table II. It can be seen that, apart from the second order transition, the exponents do not have the mean field values. Above T_c the exponent γ has a value typical of a three dimensional Ising model, rather than that of unity, c.f., equation (12). Below T_c the value of γ in the first order systems is 0.73 independent of grain size or of uranium concentration. This confirms our proposal that the transition is first order and of the same dimensionality in all the samples except those with small grains.

ii Dynamic Scaling in the low frequency response

This form of scaling establishes a relationship between the relaxation rate and the susceptibility increment in the critical region. It can be succinctly defined in the following equations which apply in the temperature region in the neighbourhood of T_c ,

$$\chi(\omega) = \chi'(\omega=0) F(\omega/\omega_p) = \chi'(\omega) - i\chi''(\omega) \quad (13a)$$

$$\chi'(\omega) \propto \chi'(\omega=0) (\omega/\omega_p)^{n-1} \quad (13b)$$

$$\chi''(\omega) \propto \chi'(\omega=0) (\omega/\omega_p)^{n-1} \quad (13c)$$

for $\omega/\omega_p > 1$ and $0 < n < 1$, with

$$\chi'(\omega=0) \propto (\omega_p)^{n-1} \quad \text{and} \quad \chi'(\omega=0) \propto |T - T_c|^{-\gamma} \quad (14)$$

One further relationship has been predicted^{9,10} and should be obeyed outside of the critical region, that is at temperatures not close to T_c . This is that

$$\chi'(\omega=0) \propto (\omega_p)^n; \quad \text{with } \omega_p \propto e^{-\Delta/kT} \quad (15)$$

The existence of both relationships (14) and (15) has been revealed¹ in the low frequency response of the samples investigated by the use of a diagrammatic technique¹¹ which constructs a master curve of the response with the functional form of equation (13a). These relationships were observed in all the samples, including sample RM35A. A typical locus of $\log\{|\chi(\omega=0)|^{-1}\}$ as a function of $\log\{(\omega_p)^{-1}\}$ is shown in figure 3. The inverse values in this plot are a result of the diagrammatic technique and have no essential significance. The particular result used in the figure was obtained for sample RM45.

It is most noticeable that in the critical regions, where equation (14) is obeyed, the branch of the locus for $T > T_c$ is separated from that for $T < T_c$, although the branches are parallel. This only arises when the crystal structure is different in the two phases, as would be expected for a displacive or first order transition. This can be demonstrated in the following manner. When equation (14) is obeyed above and below T_c we have that

$$\chi(T_c+) \propto [\omega_p(T_c+)]^{n-1} \quad \text{and} \quad \chi(T_c-) \propto [\omega_p(T_c-)]^{n-1} \quad (16)$$

$$\text{and} \quad \frac{\chi(T>)}{\chi(T_c+)} = \left[\frac{\omega_p(T>)}{\omega_p(T_c+)} \right]^{n-1} \quad T > T_c \quad (17a)$$

$$\frac{\chi(T<)}{\chi(T_c-)} = \left[\frac{\omega_p(T<)}{\omega_p(T_c-)} \right]^{n-1} \quad T < T_c \quad (17b)$$

therefore

$$\frac{\chi(T<)}{\chi(T>)} = \left[\frac{\omega_p(T<)}{\omega_p(T_c-)} \times \frac{\omega_p(T_c+)}{\omega_p(T>)} \right]^{n-1} \times \frac{\chi(T_c-)}{\chi(T_c+)} \quad (18)$$

which becomes

$$\frac{\chi(T<)}{\chi(T>)} = \frac{\chi(T_c-)}{\chi(T_c+)} \left[\frac{\omega_p(T_c-)}{\omega_p(T_c+)} \right]^{1-n} \quad \text{when } \omega_p(T>) = \omega_p(T<) \quad (19)$$

Hence this ratio will only be unity when the proportionality constants in equation (16) are identical. These must have a form such that the susceptibilities are dimensionless and will be dependent on the frequency, the density of the dipoles and their dipole moment, among other features. Expression (19) has been checked and found to be obeyed for these samples. Figure 4 gives the ratio of relaxation rates in the two phases at T_c .

It is also noticeable that the small grain sized sample shows a similar discontinuous behaviour to the other samples, although close to T_c a modification appears which results in experimental points appearing in the middle of the two parallel branches. A similar effect has been found for individual experimental points in the data for the other samples. It can be generally concluded that the observed dielectric response originates in dopant regions undergoing a first order transition which is forced by the host lattice. In addition to this the dopant regions of the smallest grain sized material will assimilate and respond together with the host lattice when the critical slowing down of the host's second order transition becomes slower than that of the dopant regions themselves.

Outside of the critical region relationship (15) has been shown to apply with both the relaxation rate and the static susceptibility following activated behaviour. In fact it can be seen that $\chi(\omega=0)$ takes the form

$$\chi(\omega=0) = (T_c +) \exp\{-n\Delta/(kT)\} \quad (20)$$

for the low dopant concentration samples (RM1A, RM35A and RM35B), figure 5.

The frequency index n arises from the coupling of the relaxation centre to the dipole reversal modes of the lattice^{4,8,12} and measures the correlation between these motions. Outside of the critical region the centre relaxes between positions separated by a potential barrier creating or annihilating a number of lattice spin reversals in the process. Such local spin reversals determine the dipole moment of the centre, but notwithstanding have as independent existence as propagating excitations on a time scale less than the relaxation time of the centres. They therefore have an equilibrium thermal population which determines the number of centres that are excited, and which gives equation (15). For example if the energy per dipole reversal is kT_c then Δ/kT_c spins are required to overcome the potential barrier. However only a fraction n of these are retained after relaxation, with n indexing the coordination of the centre relaxation with the lattice motions.

The activation energies of the susceptibility have been found to be $2kT_c$ for RM1A and RM35A, corresponding to a single ferroelectric reversal and $3kT_c$ for RM35B. A peak of $5kT_c$ was observed for the 0.6% uranium sample and a return to $2kT_c$ for the maximum concentration of 1%, figure 6. The values of the index n , as a function of concentration, follow a similar pattern which is given in figure 7. Increases in centre to lattice coupling will stiffen the higher frequency lattice vibrations because of a decrease in the ability to respond on their time scale. It is, therefore, to be expected that the

ratio of relaxation rates below and above T_c will also follow the same pattern as can be seen in figure 4.

As the critical temperature is approached the lattice dipole reversals couple strongly together with a correlation length leading to the critical phenomena¹³. At T_c all reversals within the region affected by the centre will take part and the susceptibility $\chi(T_c^+)$ will measure their number. Since the non-critical value of equation (15) measures the thermal population as a fraction of the same fixed number equation (20) results.

Increasing uranium concentration progressively damages the lattice in the vicinity of the uranium centres, as can be seen from the decrease in the activation energy of the relaxation rate, figure 8, and from the drop in T_c at the highest uranium concentrations. This is also observed in the change in the relaxation rate ratios shown in figure 4. It thus appears that some dopant clustering occurs at these highest concentrations. At 0.6% uranium (RM45) this clustering is insufficient to affect the host lattice ferroelectric couplings which determine T_c and the uranium centres therefore involve a large number of dipole reversals in their relaxation, giving a larger value of n . This stronger coupling to the host lattice stiffens the lattice itself and increases the ratio of relaxation frequencies. At 1% dopant (RM46) the uranium centres start to reduce T_c and hence must be damaging the lattice to some extent. Since $\omega(T_-)$ is much less than $\omega(T_+)$ it appears that this damage reduces the lattice stiffness through the production of vacancies. It is noticeable here that equation (20) is obeyed if $\chi(T_+)$ is replaced by $\chi(T_-)$ as if the total number of dipole reversals available within the same sized correlation region were different in the ferroelectric and paraelectric phases, possibly as a result of the low temperature lattice distortion.

Conclusions

These results reveal the phase transition for the uranium doped ceramics to be generally of first order. It is possible that this is caused by electrostriction from the unclamped grain boundaries modifying the second order displacive transition expected of the perovskite structure. The sample with the smallest grain size has been shown to revert to the second order. The detail of the main ferroelectric dispersion however could not be observed as it lay in a frequency region that was outwith the frequency range investigated.

The transition characteristics of the smallest grain sized material indicated the presence of a size effect in limiting the approach of the soft phonon to zero frequency at the critical temperature. An estimate of the effective grain size, and hence of the maximum correlation length, can be made by taking the increase in the permittivity at 10⁴ Hz in the critical temperature region as 10³ and using the observed mean field values of one half for ν and zero for η in equation (2). A value of thirty to forty lattice spacings is obtained, which is about one thirtieth of the grain radius in this fine grained material.

A dielectric response originating from the uranium and the dopant sites has also been observed. It has been shown that this response was first order in all cases. The existence of dynamic scaling relationships was verified and a new, non-critical, relationship has been discussed in qualitative terms. The uranium centres have been found to couple locally to dipole reversals in the lattice. Their maximum response at T_c appears to be determined by the number of dipole reversals available for coupling, that is by their domain size which, except for the 0.4% samples, appears to be of the order of ten lattice spacings, when due allowance is made for their concentration.

The single calcined material represents a special case in which the uranium domain undergoes a first order transition but at temperatures close to T_c it relaxes faster than a critical slowing down second order process which it then follows exactly. In this way it becomes part of the host lattice with a very large maximum response at T_c which is of the same order as that of the permittivity at 10^4 Hz. It is therefore very likely that the critical slowing down is an overdamped soft mode.

In summary it has been found that

The first order/second order classification is a consequence of a size effect and due to the volume/surface ratio of the grains. This has serious consequences for the mode structure of the material.

There is no direct evidence of a size effect in the correlated properties of the materials investigated. In all cases the correlation length was a fraction of the observed grain sizes. The correlation length has been estimated as being approximately thirty lattice spacings, that is of the order of one hundred angstroms.

References

1. M. E. Brown, Ph.D. Thesis, University of London, 1981
2. J. M. Sancho, N. San Miguel & J. D. Gunton, J.Phys.A., 13, 1980, p L443
3. T. Mitsu, I. Tatsuzaki & E. Nakamura, "Ferroelectricity and Related Phenomena", Vol 1., Gordon & Breach, New York, 1976
4. B. I. Halperin & C. M. Varma, Phys.Rev., B14, 1976, p 4030
5. R. W. Whatmore, R. Clarke & A. M. Glazer, J.Phys.C., 11, 1978, p 3089
6. A. K. Jonscher, Phil.Mag., B38, 1978, p 587
7. K. G. Wilson & J. Kogut, Phys.Rpts., C12, 1974, p 75
8. P. C. Hohenberg & B. I. Halperin, Rev.Mod.Phys., 49, 1977, p 435
9. L. A. Dissado & R. M. Hill, Phil.Mag. B41, 1980, p 625
10. R. M. Hill & L. A. Dissado, Nature, 281, 1979, p 286
11. L. A. Dissado & R. M. Hill, J.Phys.C., 14, 1981, p L469
12. L. A. Dissado & R. M. Hill, Nature, 279, 1979, p 685
13. M. de Leener, "Lecture Notes in Physics", 31 - 33, 1970 - 1975, (Int.School of Stat.Mech., Sitges, Spain), Springer-Verlag, New York, p 237

Future Work

This report completes the work that will be carried out on ferroelectric systems.

During the remaining six month period of the present contract it is intended to investigate correlated conduction processes in semiconductor materials. In particular silicon will be considered as the model semiconductor and the interaction of correlation size effects with carrier relaxation times and carrier noise will be examined. In the first instance the investigation will be theoretically based but experimental data, where available in the published literature, will be made use of.

Table I

Sample Number	Mean Grain Diameter	Dopant Concentration
RM1A	11 m	nil
PM35A	2.5 m	0.4%
RM35B	22 m	0.4%
RM45	24 m	0.6%
RM46	17 m	1.0%

Table II

Critical exponents for the ferroelectric, high frequency, process
below and above T_c

Sample Number	$\epsilon_\infty \approx (T_c - T)^{-\gamma}$	$\epsilon_\infty \approx (T - T_c)^{-\gamma'}$
	γ	γ'
RM1A	0.74	1.25
RM35A	1.0	1.0
RM35B	0.73	-
RM45	0.73	1.4
RM46	0.73	-

Legends

Figure 1. Arrhenius plot of the zero frequency susceptibility of the ferroelectric, high frequency, process. The discontinuities characteristic of first order transitions are indicated by the dotted vertical lines.

Figure 2. Plots of the permittivity at 10^4 Hz and the magnitude of the low frequency response close to T_c as a function of the concentration of the uranium dopant

$$\epsilon_{\infty} :- \times T > T_c; \circ T < T_c : A(T) :- + T > T_c; \square T < T_c$$

Figure 3. Temperature datum trace for sample RM45 showing the critical branches of gradient -0.65 and the non-critical branches of gradient 0.37. The correlation index n of this sample was measured as 0.35 from a frequency plot of the susceptibility. The direction of temperature increase is shown by the arrow heads.

Figure 4. Relaxation rate ratio as a function of uranium concentration

Figure 5. Arrhenius plot for the inverse susceptibility of sample RM35A. Note the infinite temperature extrapolation of the activated regions.

Figure 6. The correlation index n as a function of dopant concentration.

■ single calcined sample; × double calcined samples

Figure 7. The activation energy of the susceptibility as a function of uranium concentration

Figure 8. The magnitude of the activation energy of the relaxation rate as a function of the uranium concentration.

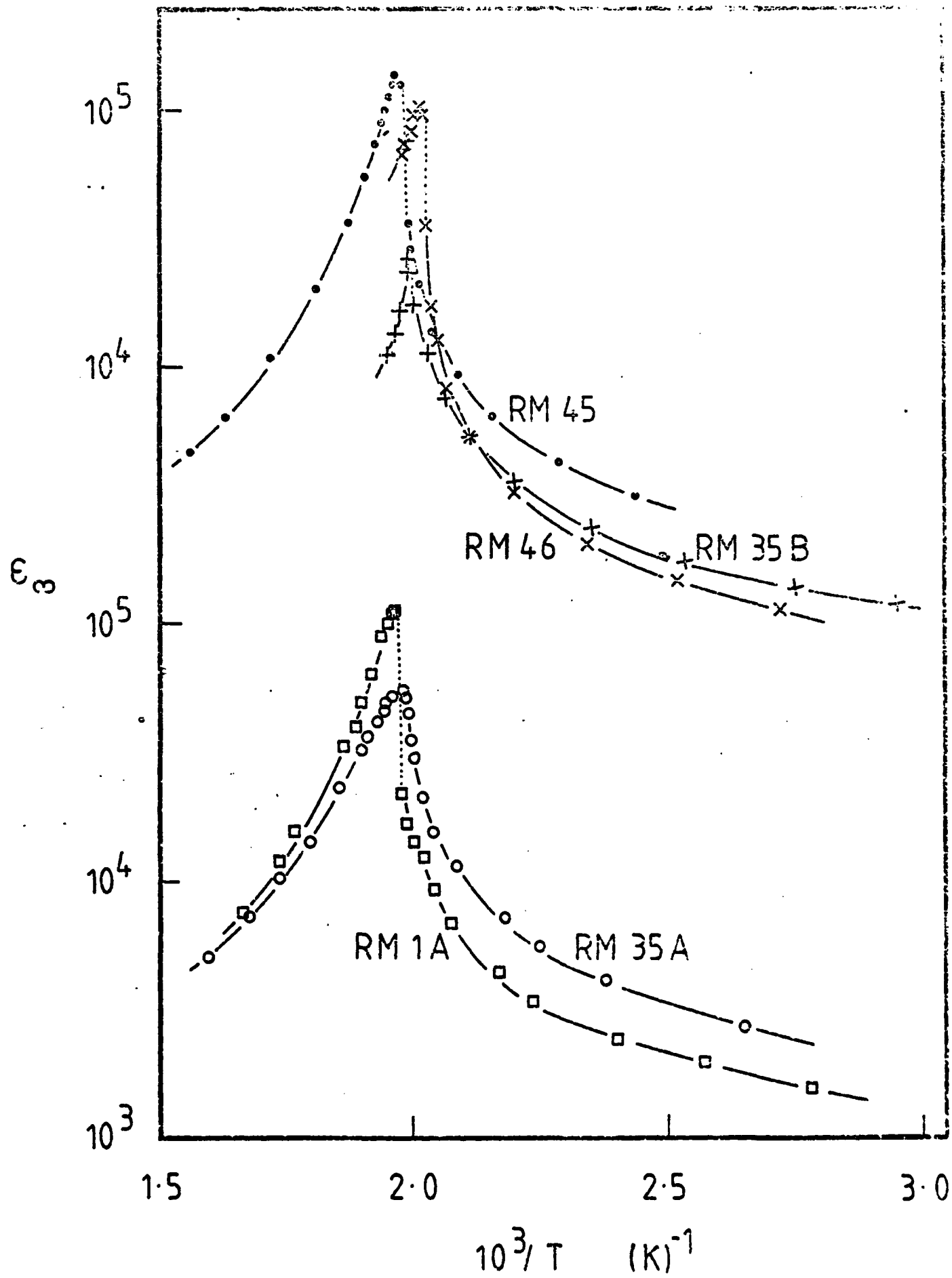


Figure 1

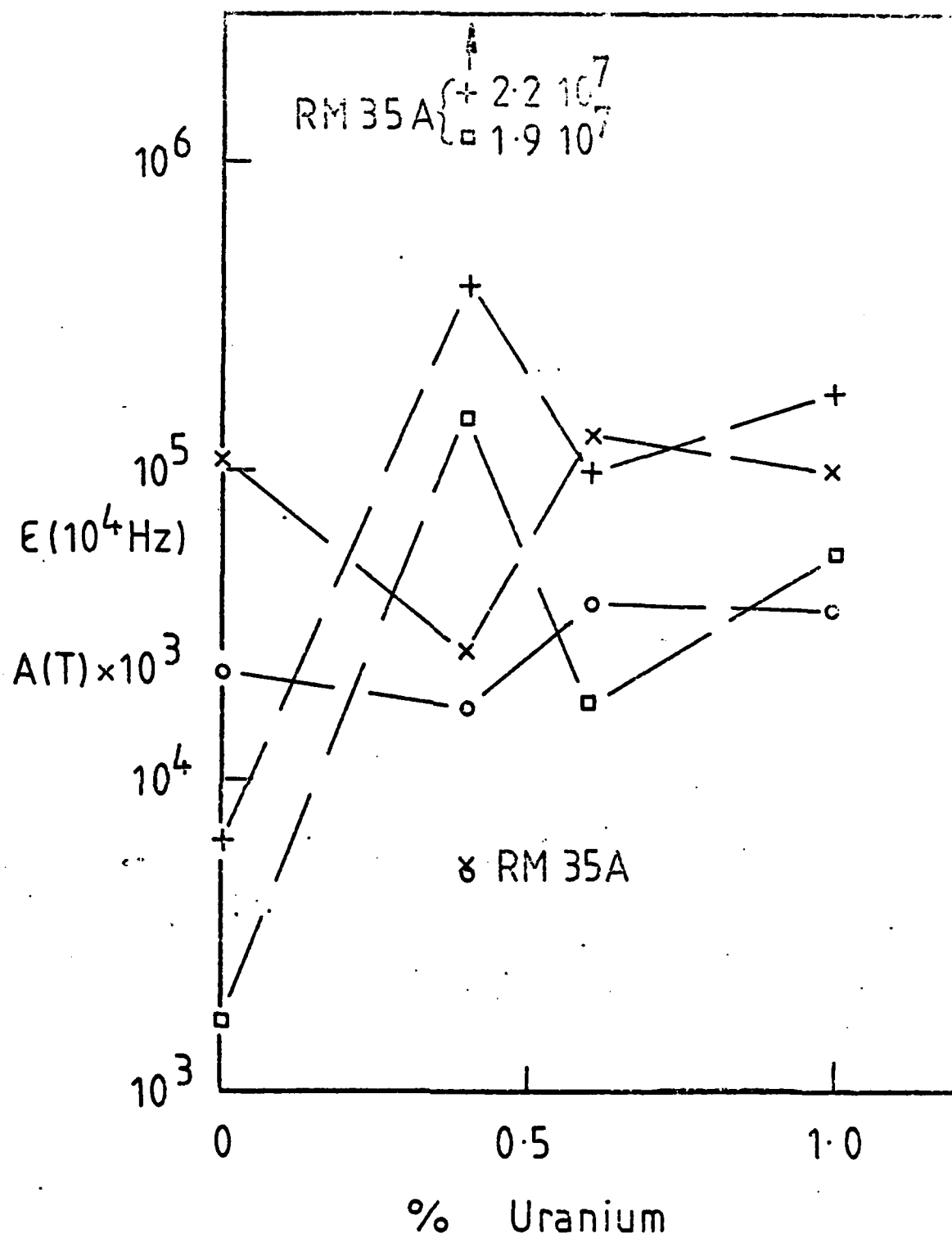


Figure 2

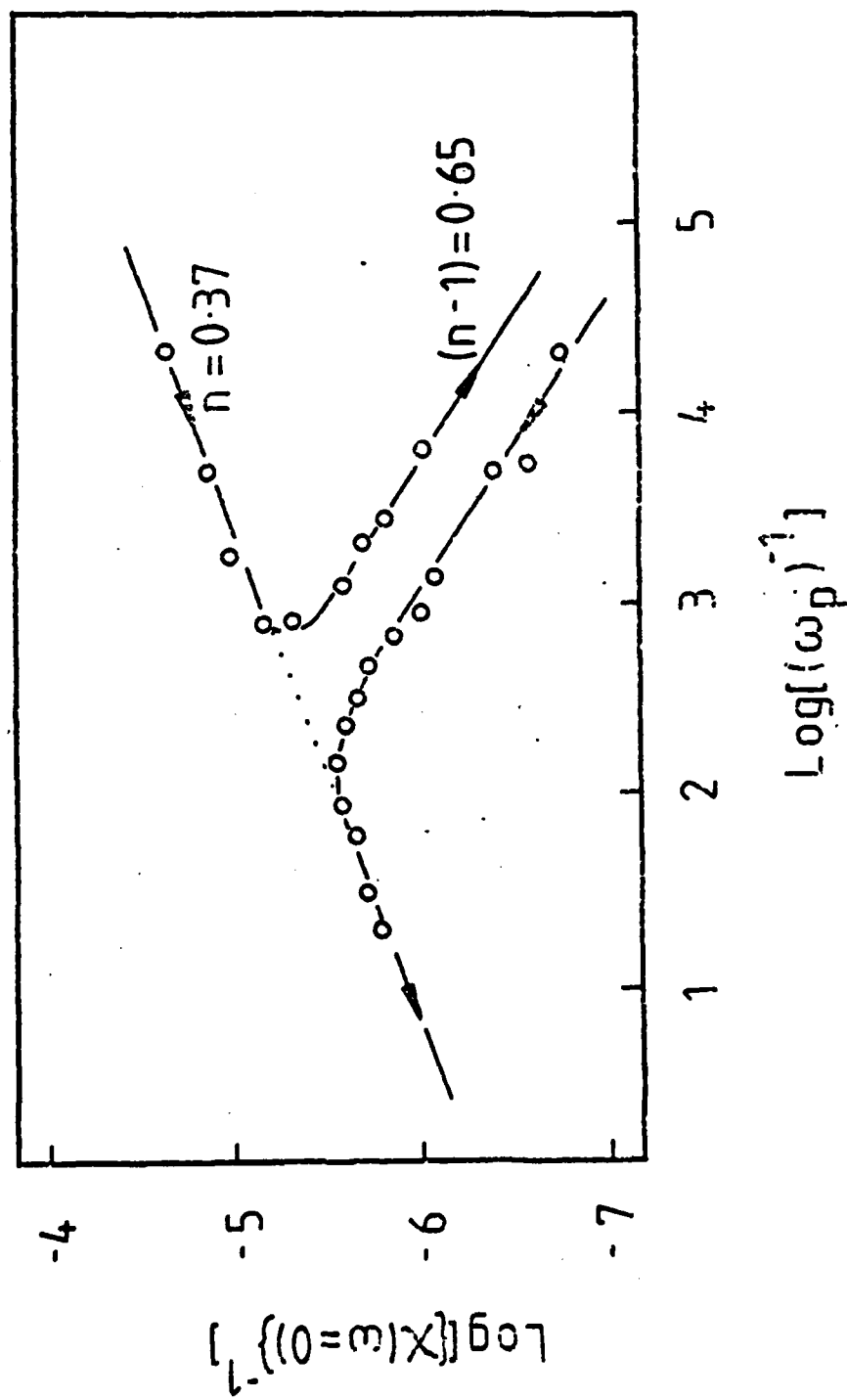


Figure 3

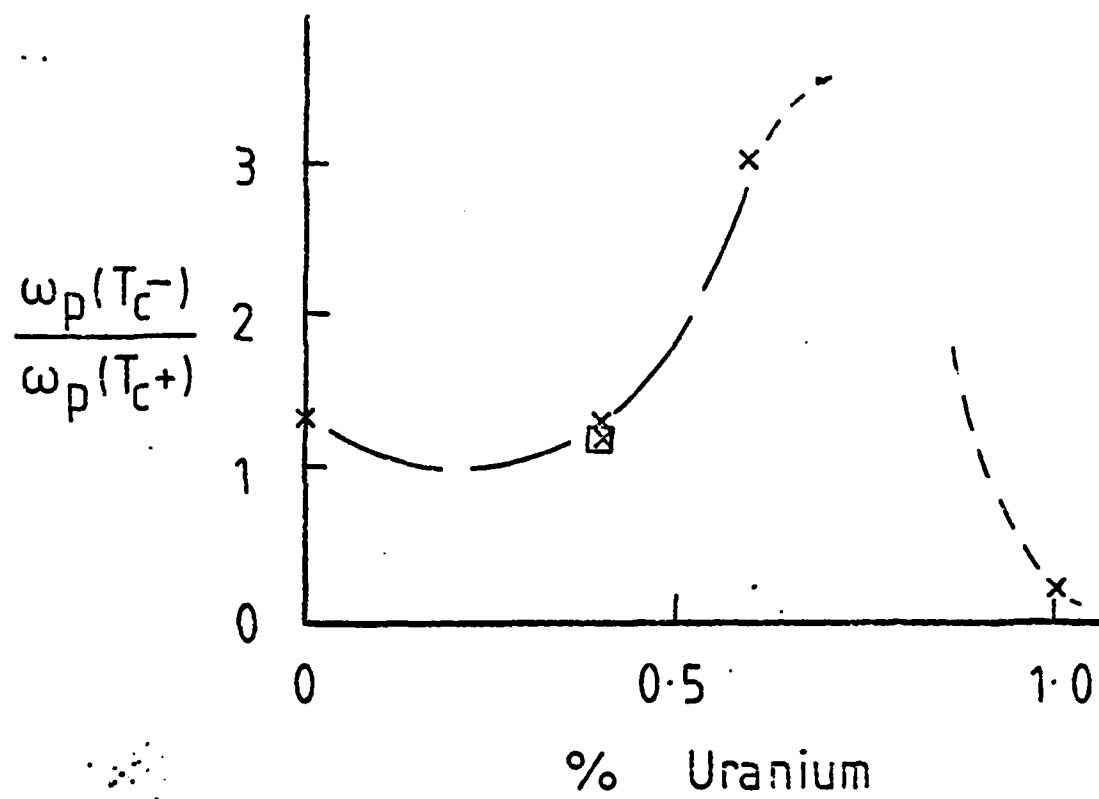


Figure 4

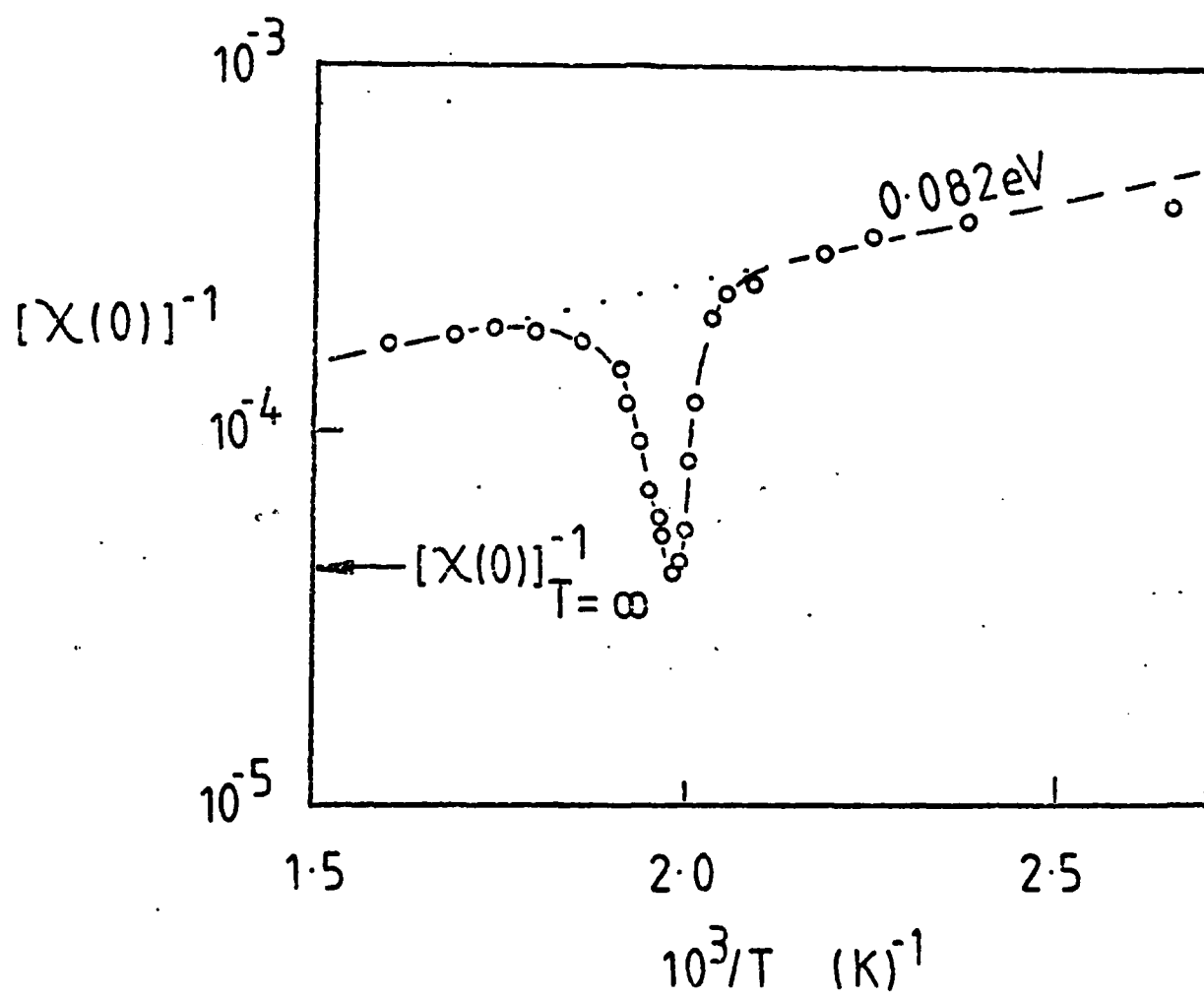


Figure 5

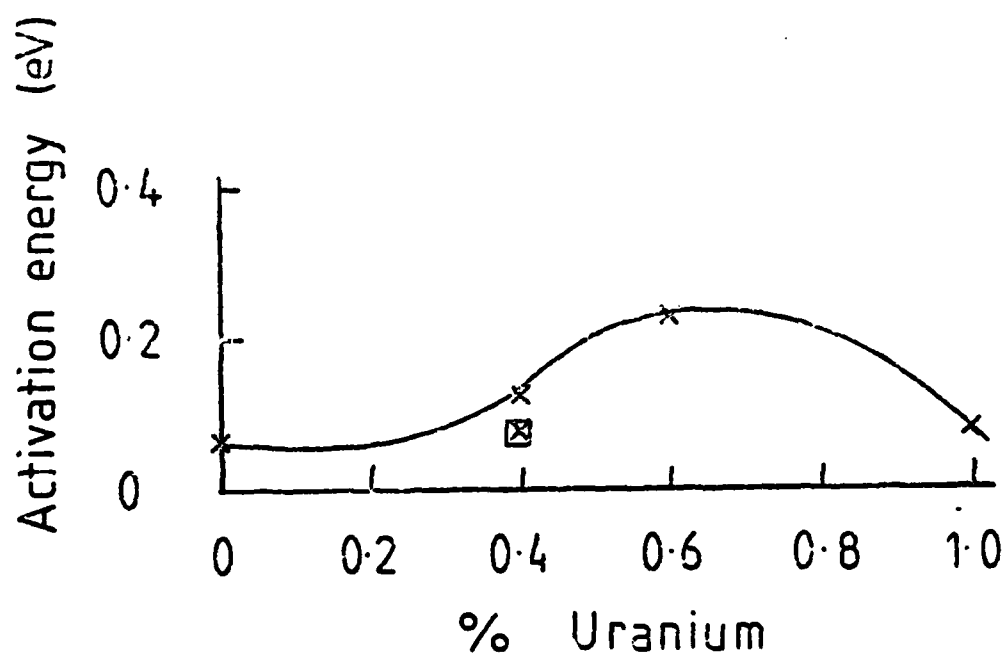


Figure 7

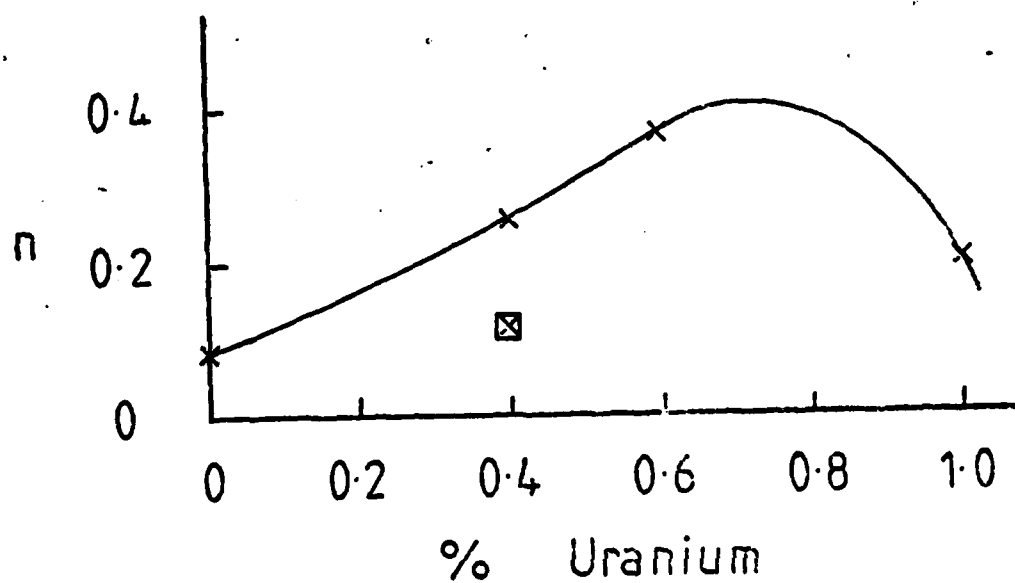


Figure 6

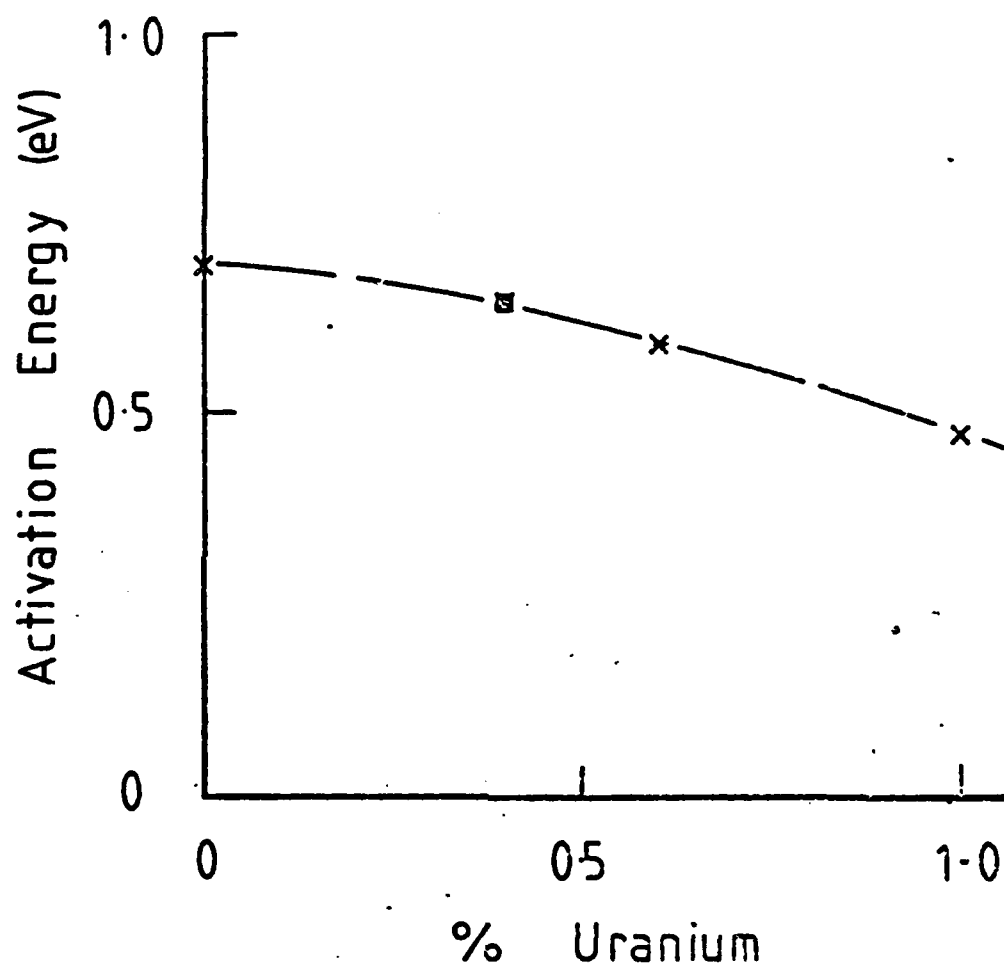


Figure 8

END

FILMED

1-83

DTIC